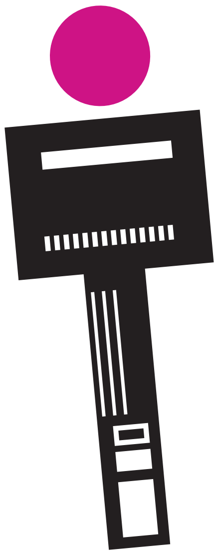

RAM ROBOTICS AND MECHATRONICS

CHARACTERIZATION AND TESTING OF A NOVEL RELIABLE METHOD TO CONNECT METALLIC AND 3D-PRINTED POLYMERIC CONDUCTORS

V. (Vinod) Ravi

MSC ASSIGNMENT

Committee:
prof. dr. ir. G.J.M. Krijnen
ir. A.P. Dijkshoorn
dr. ir. D. Alveringh

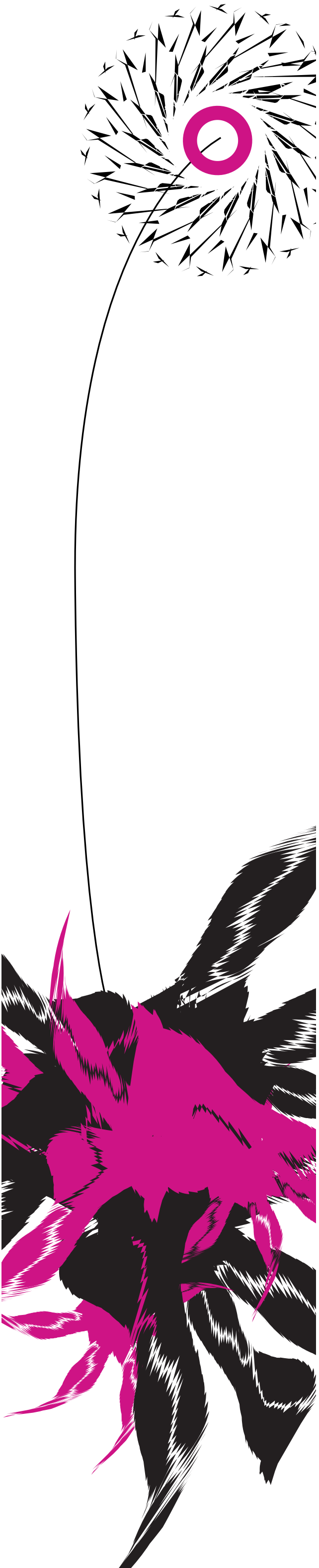

December, 2023

058RaM2023
Robotics and Mechatronics
EEMCS
University of Twente
P.O. Box 217
7500 AE Enschede
The Netherlands

UNIVERSITY OF TWENTE. | TECHMED CENTRE
UNIVERSITY OF TWENTE. | DIGITAL SOCIETY INSTITUTE

Summary

With 3D-printing gaining momentum in the fabrication of flexible electronics, there is a need for a reliable method to connect metals and conductive polymers both electrically and mechanically as flexible 3D-printed electronics would require connecting to a metal conductor to interface with standard electronics. In any practical application, flexible electronics require connection with a metal conductor to interface with standard electronics. This research investigates a novel approach to connect metallic and 3D-polymeric conductors using mechanical interlocking to characterize and test the mechanical and electrical behavior. Mechanical interlocking is achieved through embedding perforated copper tape during the 3D-printing process, in order for molten electrically conductive Thermoplastic Poly-Urethane (ETPU) to extrude through the perforations. The physical sample is modelled to obtain desired electrical performance metrics and fabricated in order to identify the optimal contact design to produce the best interlocks. An experimental setup is fabricated to accommodate this sample in order to perform tensile tests to evaluate simultaneous mechanical and electrical performance of these contacts, simulating their potential real world applications. Behavior of contact resistance and breaking points of copper tapes are observed for uniaxial and cyclic tensile loads.

The results showed that perforated tapes create mechanically stronger contacts than conventional wires. Contact resistance is observed to be relatively low and stabilized under large periodic loads. More experiments along with comparisons to existing contact methods are required for statistically significant results. The current hypothesis for why the contacts work well with mechanical interlocking lies in the mismatch amongst thermal expansion coefficient between copper and ETPU could promote shrink fit, thereby increasing effective contact area between materials. The improvements with regards to fabrication, design parameters and extensive testing in this research aid to the evolving field of additive manufacturing of flexible electronics and sensors by addressing critical challenges in bonding electrical components to 3D-printed structures, but also towards standardizing one such method. Applications could revolve around flexible, stretchable and conductive objects, as part of soft robotics and biomedice. Wearable sensors that measure physiological signals, robotic prostheses which emulate flexible limb behaviour like grasping and manipulation and skin/clothing integrated displays, to name a few.

Preface

This thesis is a research venture on how to improve a novel but reliable method to connect metal with 3D-printed conductive polymer, with a hope to getting closer to standardize this method. Although, I initially hoped to identify a newer solution. This open ended search was not successful due to complications and an even more tumultuous 2021. Nevertheless, this allowed me to explore further into understanding, simulating and fabricating an existing mechanical system, to utilize creativity in fabricating my own tools and a testing rig, in order to aid and experiment. Ever since I obtained newfound pleasure working on mechanical aspects at my internship at Roetz Bikes, this project further availed me an opportunity to help me venture more towards the mechanical aspects, as I have always dreamt to shape my future endeavors.

This journey through its highs and lows, culminating with the attainment of a diploma from University of Twente, could not have been possible without the support of many benevolent people I encountered along the way.

First and foremost, my heartfelt thanks go to Professor Gijs Krijnen, for your unwavering support, prompt responses to every update/query well outside office hours, empathizing with my personal struggles but also being honest with what needs to be done. The biweekly discussions always helped me obtain more clarity about the immediate tasks and aided me in navigating my way. Thank you for your dedicated commitment to harboring a passion for research and learning. To Alexander Dijkshoorn, thank you for your patience, expertise and continuous encouragement, all of which have been cardinal in transforming challenges into opportunities for growth. Your role was crucial in shaping the direction of my thesis, providing constructive feedback and for helping me realize that sometimes a solution can be simple without unnecessary complications. Importantly, your mentorship extended beyond its technical aspects, allowing for me to express personal difficulties and gaining your perspective, which was instrumental in obtaining a resurgence in my own workmanship.

Beyond academic support, I am thankful for the new (unexpected but welcome!) friendships that were forged during this journey. For being an introvert all my life, I am elated to finally realize the quality of life improvement from having people in my circle. I am indebted to these passionate individuals who stood by me during difficult times and gifted me incredible memories on my journey. I extend an honorable mention to my Calslaan neighbor Vishal, from providing my first meal in the Netherlands to making me feel at home in a new country. You never failed to add humor and joy to my days, from discussing about aircrafts to making Şalgam as the official post dinner ritual drink. Navigating life in Enschede outside the campus was enriching. My gratitude extends to Valentin, for being an amazing roommate but an even greater friend to my father, who enjoyed the camaraderie with your gang of friends and reminisces it even today. I look forward to performing music on the same stage with you. Atif, your hospitality knew no bounds. Your tales of life in Tunisia and helping me experience home cooked Tunisian cuisine, were invaluable.

I'm extremely grateful for the newfound family amongst Bas, Lian, Mees, Marit, Petra, Sjors and Talia. Learning more about the Dutch & Belgians and their cultures can be one thing, but being an active participant in their lives has been wholesome. Their effort to include me to be a part of their life and eagerness to see me again, has been overwhelming. It was surreal how back when 'Ik spreek een beetje Nederlands', I never felt out of place when they spoke amongst each other in Dutch. They've all added quality to my life in the Netherlands.

In memory of Shreyas, who brought constant laughter, a sense of brotherhood and a shared love for the anime: Dragon Ball Z. You will always be remembered for the positive impact you've had on more people than you realize.

To Balaji, who has been my oldest friend and a brother since 2006, I absolutely cherish the life talks we had at 3am while we gamed mindlessly. Its funny how we normally find it hard to make time to talk due to conflicting schedules but its always easy over a game of Call of Duty. To Mohith, I have no words to describe how much impact you've had over the last decade with regards to my life. I absolutely enjoy our hour long conversations about video game lore over delectable South Indian cuisine. You always looked out for me, even half the world away.

A special mention to Arwa, whose unfaltering support, understanding, and love have been my constant motivation. Your presence has been a staggering source of strength and your efforts to figure out solutions to reduce any shred of stress upon me, have been a blessing. I will continue to cherish all the shared moments that made my journey memorable while eagerly looking forward to the future.

Undoubtedly, this section would be incomplete without expressing gratitude to my family. I thank my parents, Ravi and Sunitha, for their everlasting and wholehearted support all throughout my life. Even as I worked from home in 2023, against challenging odds and financial conditions, you always took care of me and tried your best to never place any burdens on me. I am here only because of the incredible hard work and sacrifices endured by both of you. Thank you for having faith in me through the ups and downs in this journey, for the utmost care provided when my health failed and for eternally being a source of love. I cannot overlook my sister, Shreya whose banter, memes and skits, always transported me to a realm of laughter and promises to look forward to. Her active involvement in singing and as an upcoming doctor, serves as another marvellous source of inspiration and pride. Any achievement that I am part of, is as much hers as it is mine, and I am truly grateful for her presence as one of my closest confidante.

In summary, I relished my time in the Netherlands and express my gratitude to everyone who contributed to the realization of my thesis. What began as a quest for a degree has clearly evolved into cherished memories and obtaining newfound family amongst people half the world away.

Vinod Ravi
Bangalore, December 22, 2023

List of Abbreviations

AM Additive Manufacturing

FDM Fused Deposition Modelling

PI-ETPU Palmiga Innovations Engineered Thermoplastic Polyurethane

ETPU Engineered Thermoplastic Polyurethane

SCF Stress Concentration Factor

CAD Computer Aided Design

IMDJ Injection Molded Direct Joining

PLA Polylactic Acid

EPLA Electrically Conductive Composite Polylactic Acid

FLEPS Flexible and Printable Sensors an Systems

Contents

1 Introduction **1**
1.1 Context . . . 1
1.2 Pioneering Work . . . 2
1.3 Problem Statement . . . 2
1.4 Goals and Reseach questions . . . 2
1.5 Report Structure . . . 3

2 Scientific Background **4**
2.1 Adhesion among materials . . . 4
2.2 Adhesion between Dissimilar Materials . . . 5
2.3 Mechanical interlocking for metal and polymer connection . . . 6
2.4 Previous work by Neuvel . . . 8
2.5 Conclusion . . . 9

3 Design And Modelling **10**
3.1 Design Requirements . . . 10
3.2 Basic Sample . . . 13
3.3 Modelling . . . 14
3.4 Revised Sample Design . . . 20
3.5 Conclusion . . . 20

4 Materials and Fabrication **22**
4.1 Introduction . . . 22
4.2 Materials and Equipment . . . 22
4.3 Electrical contact fabrication . . . 25
4.4 Final samples . . . 28
4.5 Conclusion . . . 29

5 Experimental Setup And Measurements **30**
5.1 Introduction . . . 30
5.2 Setup Concept . . . 30
5.3 Components . . . 30
5.4 Measurements . . . 33
5.5 Conclusion . . . 36

6 Results **37**
6.1 Introduction . . . 37
6.2 Mechanical interlock interface . . . 37

6.3 Uniaxial Loading Measurements 37
6.4 Cyclic loading measurements 46
6.5 Conclusion 48

7 Discussion **50**
7.1 Copper tape versus copper wire 50
7.2 Role of the perforations 50
7.3 Difference in thermal expansion between ETPU and copper 51
7.4 Contact points between copper and polymer during pulling 51
7.5 Failure point scenario 52
7.6 Estimation of R_{3D} 52
7.7 Behavior of resistance during pulling 54
7.8 Conclusion 56

8 Conclusion and Recommendations **57**
8.1 Conclusion 57
8.2 Future Recommendation 58

A Appendix 1 **60**

Bibliography **61**

1 Introduction

This report describes the work done by Vinod Ravi for the final assignment of his Master in Electrical Engineering. The goal of the assignment is to characterize and test a novel method to connect 3D-printed polymers to metallic conductors. The samples produced by utilizing this method will be used to study the mechanical and electrical behavior of the system.

This chapter introduces the context for the study along with the challenges involved, followed by the questions that will provide a basis for the goals of this research. Finally a global overview of the entire report structure is provided.

1.1 Context

The rapid advancement of additive manufacturing (AM) techniques including Fused Deposition Modelling (FDM), direct metal depositing and selective laser sintering have revolutionized the fabrication of complex and functional components, extending beyond the realm of static objects to dynamic and interactive devices. The systems vary in the materials they can reliably fabricate and the way they build their structures [1]. Printed formations now incorporate electrical and electronic components, expanding the capabilities of 3D printing further than the fabrication of static components with complicated geometries and into the creation of functional units that can move, perceive, and compute. Interconnected electromechanical gadgets and structural electronics, with in-built sensing devices, actuators, interlinks, and possibly processors and power supplies, are the next technological advancement for 3D printing, and they can be printed automatically in a single console [2]. In expanding the scope of design possibilities for innovative products and to enable functionality that is not feasible with traditional processes, such 3D-printed devices could allow designers to build sophisticated working mechanisms with a greater extent of customization. Monolithically manufactured, decentralized actuators and sensor systems can improve the sturdiness and flexibility of 3D-printed robotic devices, specifically, soft robots [3]. This is because it allows for greater control across numerous degrees of freedom of motion, which in turn allows for more intricate motions as well as shape changes, greater dexterity, and greater system robustness via redundancy. A 3D-printed unified electromechanical gadget has many uses beyond robotics, including in defence systems [4], innovative prosthetics [5], wearable technologies [6], embedded strain-sensing devices [7], and individualized consumer devices [4].

Because of its capacity for creating geometrically complex parts smartly and safely in an office-friendly surrounding, 3D printing approaches, especially FDM, has seen widespread use in AM techniques that offer functional prototypes in a variety of materials. Most of these applications require the bonding of electrical wires to the 3D printed parts. Getting electrical wires to bond to these conductive prints is difficult because the contact resistance is highly dependent on the type of connection used [8]. Current systems are either better suited for rigid 3D-prints than flexible, deformable applications or have uncontrollable material characteristics and reproducibility. More so, there is a dearth of research on how the bonding technique impacts the contact resistance [9, 10]. Amalgamation of metallic conductors with conductive polymers clearly opens up a spectrum of applications that demand diverse properties in conjunction: Electrical conductivity, mechanical strength, flexibility and deformation durability. Commonly explored solutions with regard to connecting metal and polymer revolve around mechanical interlocking, adhesives, melting, soldering, welding and pressure contact.

Given the diverse range of applications that require these electrical connections, it is imperative to define a set of standards to ensure reliability, quality and compatibility. This standard should address compatibility of materials for their unique properties and long term stability. It should

also offer design recommendations for creating effective and durable connections providing guidelines on joint geometry and distribution of stress along the interface. Testing protocols can be established further to evaluate the performance of metal-polymer connections namely, electrical conductivity, mechanical loading and durability assessments under cyclic loading. This would pave way for a standard to outline quality control procedures to ensure that fabricated products indeed adhere to defined specifications. This is crucial for applications in sectors like healthcare [11] and aerospace, where safety and reliability are paramount.

1.2 Pioneering Work

The foundational basis for this project is based on another research pursuit towards establishment of a dependable method to achieve a reliable connection between metallic conductors and conductive polymers carried out in the NIFTy group by Patrick Neuvel [12]. The outcome of this research revealed that polymer tracks printed over perforated copper tape demonstrated the ability to withstand a simple pulling force. Polymer had effectively been extruded through holes and fused with a underlying base layer. This lays the groundwork for choosing mechanical interlocking with its first steps towards a promising approach to a achieve a reliable connection between dissimilar materials. Currently, solutions for connecting dissimilar materials like metal and polymer fall short in standardization, adhesion enhancement, durability, flexibility and cost. Both adhesion and durability are paramount to be assessed for the long term performance in extreme conditions.

1.3 Problem Statement

Within the nascent realm of 3D-printed electronics, a significant challenge arises when it comes to effectively connecting dissimilar materials like metal and polymer, especially elastomers [13]. While metals offer excellent electrical conductivity and mechanical strength, polymers provide the advantage of flexibility, deformability and light weight properties. However, due to their limited mutual solubility and the stark contrast between the chemical and mechanical properties, these virtues of individual materials become a hurdle in creating a stable, durable and conductive connection between them [14]. Securing metal with polymers can also lead to stress build-up and mechanical failure arising from disparity in mechanical and thermal properties [15]. While there is no dearth of bonding techniques described in the literature, there is no one agreed-upon method. Methods such as exerting pressure to a PCB or contact [16] and application of glue with silver paste or epoxy [17] are widely used. These are typically utilized for rigid 3D-prints and are not predominantly ideal for flexible or deformable components. Surface treatments, such as plasma surface activation and chemical methods [14], can improve adhesion but add inherent complexity to the 3D printing procedure. Mechanical interlocking is a solution for securely joining materials with different properties. When metal and polymer are joined using mechanical interlocking formation, the joint strength is not affected by the weak adhesion at the interface but rather by the structures and their inherent material properties themselves [18].

1.4 Goals and Reseach questions

The cardinal objective of this master thesis is to characterize, potentially improve and quantify both mechanical and electrical performance metrics by testing. The basis of this begins with understanding the novel interlocking mechanism explored by Neuvel [12]. The first goal is to design a sample and model it with regards to the desired performance metric under study. The second goal is to implement the novel method and attempt to improve upon the build of the sample. Finally to design an experimental setup to install the sample onto, in order to simultaneously measure the electrical and mechanical performance.

To achieve the goal of characterization and improving upon a novel method to secure conductive 3D-printed polymers to metallic conductors, the following research questions are defined:

- What is the motivation and evidence behind the novel method involved in connecting 3D-printed polymers to metallic conductors, and how can this be characterized with regards to FDM?
- How can a physical sample employing this connective method be modelled in order to define the desired mechanical and electrical performance?
- What are the factors to be considered in design and fabrication of a sample employing this connective method?
  - How to optimize electrical conduction alongside ensuring mechanical strength between conductor and polymer?
  - How do printing parameters influence the electrical and mechanical properties of the sample?
- How can an experimental setup be designed to measure both electrical and mechanical properties?
- What happens to the resistance during loading/breaking point?
- What are the mechanical failure mechanisms of these connections?
- What are the insights obtained from the results and observations that can aid the advancement of mechanical interlocking as a standardized, stronger and more reliable method to secure metallic conductors with conductive polymers?

1.5 Report Structure

Successful execution of this project presents several intricate challenges. These challenges encompass understanding the connective mechanism, creation of a sophisticated equivalent model capable of accurate representation, fabrication of a sample and establishment of a measurement configuration to quantify its characteristics. Consequently, this document is structured to address each of the aspects individually, with each stage building upon the outcomes of the preceding work. Chapter 2 introduces an overview of the theoretical background and highlighting currently explored solutions relevant to this. Chapter 3 provides the design choices taken into consideration for conceiving a mechanically interlocked polymer-metal sample. Chapter 4 provides the essential details for a fabrication process along with the parameters involved. Cumulative findings from the preceding two chapters lead to the experimental setup and the measurements performed, all of which are explained in Chapter 5. In Chapter 6 the results of these measurements are analysed. Lastly, the report is concluded in Chapter 7 with the findings discussed, along with recommendations for future studies which could pave way one step closer to a quantifiable standard method to form a metal to conductive polymer connection onboard flexible electronics.

This report presents the work conducted as part of Vinod Ravi as part of his Master's Thesis. The research methodologies followed, interpretations explained, experiments performed and findings presented in this report have also been published as co-authored in "Mechanical Interlocking for Connecting Electrical Wires to Flexible, FDM, 3D-Printed Conductors" [19], as part of 2022 IEEE International Conference on Flexible and Printable Sensors and Systems (FLEPS). This report holds content that is largely based on the work published in cited paper [19]. This is honestly stated to maintain transparency and avoid issues that can arise from self-citation and plagiarism. Please also refer to the paper accordingly for any similarities noted.

2 Scientific Background

This chapter presents a relevant theoretical background of joining materials followed by a specific focus on connecting metals and polymers as dissimilar materials. An emphasis on utilizing a specific method called Mechanical Interlocking is introduced and followed by a discussion of how 3D-printed conductive polymer onto modified metal conductors can cause a mechanically interlocked joint which is mechanically reliable alongside electrical conducting. Along with a discussion of similar research carried out, the previous work done by Neuvel [12] in regard to this is introduced, which serves as a basis for this research to improve upon.

2.1 Adhesion among materials

Adhesion, from Latin for 'to stick", is the root of this term [20], and adhesive bonding is widely used in contemporary manufacturing processes [21]. Adsorption principles, bonding through chemicals, diffusion, electrostatic attraction, mechanical interlocking and weak boundary layer theory are few of the hypothesized causes of adhesion. However, there is no a single concept that is able to provide an exhaustive justification for all kinds of adhesive interaction and connectors [22]. The bonding procedure may involve particular surfaces, chemical treatments, different mechanisms, specific environmental conditions and/or combinations of them.

According to ASTM International's D 907-04 standard, adhesion is defined as a state where two surfaces of individual materials are held together by interface forces which may result from chemical bonding or interlocking or both [23]. The potency of joining is dependent on multiple properties like the surface energy of the individual materials and roughness [23]. Generally, this process is utilized to combine individual parts together into a singular structure to achieve a desired physical performance.

2.1.1 Types of Adhesion Mechanisms

Presently, there is no standard global model that explains all the occurring physical processes at the interface between two joining materials. Different adhesion mechanism theories from literature are briefly discussed to help understand the underlying phenomena and to bring focus to one of these mechanisms later on, based on which this research is undertaken [24].

Chemical Bonding

Adhesion in two surfaces in proximity can occur from molecular bonding. Chemical bonding can include various forms e.g. covalent, ionic and metallic bonding. This form of bonding requires specific compatible materials alongside proximity in order to react chemically and this type of bond is also referred to as primary Bond.

Physical Adsorption

Two materials can also be joined due to intermolecular Van der Waals forces. This bond is comparatively weaker than primary bonds and yet is sufficient to support integral structural loads when there is a large number of such interactions in a system [25].

Electron sharing

Electronic adhesion theory was proposed by Derjaguin [26] which describes sharing of electrons amongst materials in contact due to varying electronic band structures. An electrostatic charge force in the form of an electrical double layer is formed at the interface which adheres the materials. When materials are separated, the electrons return to their original states and thus the electrostatic force is reduced. This theory is supported by the observation of electri-

cal discharges when some adhesive bonds are broken. Electrostatic component of adhesion is smaller than the physical adsorpotion due to Van der Waals forces [26].

Diffusion Theory

Adhesion is due to the movement of repeating macromolecules/monomers of two polymeric materials at their interface, which is referred to as diffusion theory [27]. Movement of monomers from one polymer to another across their interface on a molecular level is classified as diffusion. This mechanism can be seen as a mechanical form of adhesion, it has been observed that Van der Waals intermolecular forces contribute to increasing adhesion [27, 28].

Mechanical Interlocking

First introduced by McBain and Hopkins in 1925 The mechanical interlocking theory discusses the idea that adhesives can flow into surface morphological irregularities on the substrate surface [29]. The irregularities can be pits, holes or craters, where the adhesive penetrates and conforms, thus enhancing the bond strength.

2.1.2 Events occurring at the interface during adhesion

Having a basic idea of the types of adhesions occurring amongst materials, a closer look can be taken at the interface during contact. Two surfaces coming to contact cause a large number of phenomena which are directly used in engineering applications involving structural adhesives, protective coating, the friction of tires and lubrication. However, the phenomenon is not completely understood [30].

Surface morphology is crucial for understanding material behavior in contact, influencing frictional heating, wear and tear, adhesion, electrical conduction, thermal swelling and electrochemical reactions. Even seemingly smooth surfaces exhibit microscale roughness, visible under a microscope. Upon contact between materials, these irregularities termed as asperities also contact one another, thus play a key role in mechanical adhesion and electrical conduction.

Modelling the real area of contact at the interface between two materials squeezed together has been an ongoing challenge [31]. The true area of contact is significantly smaller than the visibly apparent contact area. When current is conducted between these materials, it is scattered across a significant number of micro-contacts which occur at a variety of regions and geometries at the interface.

Additionally, this also causes electrical contact resistance, which arises due to the true contact area, which again relies on the size and spatial distribution of sperities in contact. Contact resistance is necessary to be considered in our research as one of the goals involves establishing electrical conduction [32]. Narrowing the focus to the type of materials involved in the research can help in taking individual properties into account, which can also help provide an idea for the type of adhesion that would be best suited for a mechanically reliable connection.

2.2 Adhesion between Dissimilar Materials

Over the years, there has been a nascent need for lightweight and high-performance engineering structures housing an increasing number of functions in individual parts which can be conceived by incorporating various materials into a multi-material joint structure.

To be able to join dissimilar materials, constituent selection, joint design and the process should equalize the challenges. Messler describes that differences should be attempted to be reduced, by making optimal choices with regards to materials or other influential factors [33]. Understandably, this gets challenging amongst different levels of involved materials' atomic, micro and macro structure levels. Differences in chemical, thermal and physical properties like

thermal expansion, fracture point, and elasticity can create problems that can compromise this bond [13, 14].

2.2.1 Adhesion of Metal and Polymer as Dissimilar Materials

Polymer metal structures are being increasingly utilized in several engineering arenas, primarily because of the potential for their associated weight savings.

It is essential to consider the individual properties of metal and polymer which can reveal the difficulty in adhering them together. Metals are well known for their durability, strength and conductivity, among others. Polymers can be flexible, versatile and in some applications, regenerative [34]. Polymers considered in this study are thermoplastics, which become soft and moldable upon raising their temperature and undergo hardening upon cooling. It can be inferred that while they are dissimilar materials, they are complementary in terms of functionality. Plastics have seen an increase in applications in engineering structures for their advantages stemming from low weight and ease of fabrication. Applications in construction, automobiles and aerospace have always demanded materials which are stronger, and stiffer but lighter.

Metal-polymer hybrid structures can ideally exploit the strength and stiffness of metals alongside functional integration and lightweight provided by polymers.

The poor adhesion can be addressed with the application of plasma treatment, but is not considered due to the complexity involved alongside 3D printing [14, 24].

While adhesive joining techniques are mostly employed in connecting metals and polymers, their main limitation involves low mechanical strength alongside extensive surface preparation [35]. There has been a nascent interest in utilizing welding in the form of laser-induced local heating, friction welding and ultrasonic welding [35], however, the individual shapes and sizes of the material constituents can pose restrictions and complexity when utilized alongside the process of 3D printing polymers while controlled thermal energy is to be strictly imparted only at the interface, which can otherwise lead to a complete failure of joining [36].

Considering these challenges amongst adhesive joining and welding techniques, mechanical interlocking emerges as an alternative. This offers the potential to overcome these limitations by taking advantage of inherent properties of the materials involved. This opens up a field of nascent possibilities in the field of metal and polymer bonding.

2.3 Mechanical interlocking for metal and polymer connection

Mechanical interlocking can cause enlargement of the interfacial contact area over which Van der Waals forces act between materials. It could also influence additional secondary forces at the interface which consist of frictional force, chain entanglement for molecular scale interlocking and mechanical forces for nano to macro level interlocking. Together, they all can aid in enhancing interfacial strength [37].

A natural solution to connecting dissimilar materials is observed amongst rigid tree roots which are interlocked in soft soil as seen in Figure 2.1, which have inspired the design and fabrication of stretchable electronics [38]. Alternatively, using the surface features of the materials can be a solution when the materials are incompatible [39]. Interlocking occurs due to features like hooks, surface roughness, pits, dimples and related surface irregularities of one material that are infiltrated or connected by the other, which have been shown to improve bonding [40].

While there have been considerable efforts towards achieving high bonding strength between metals and polymers, solely involving mechanical interlocking is fairly low. There have been numerous experiments that are starting to make headway with this approach. Park et al. have experimentally demonstrated the promising approach to utilizing mechanical interlocking to address material limitations [41]. Sancaktar et al. prepared micro-geometries through sand-

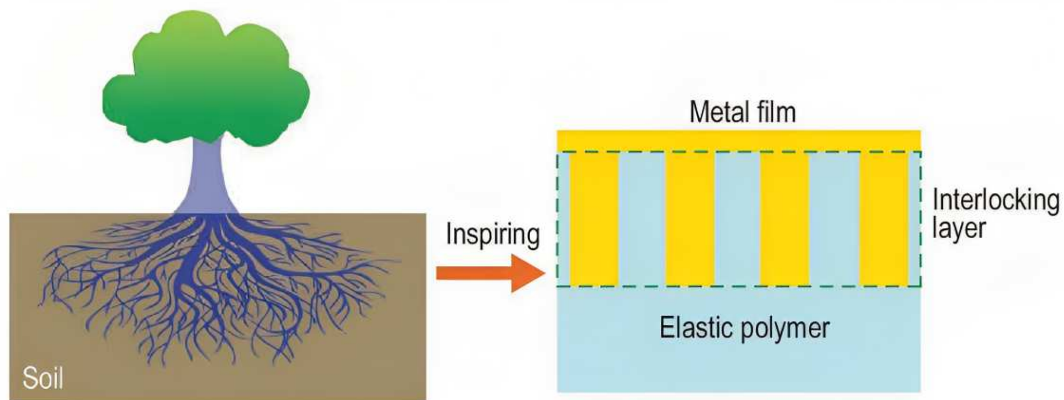

Figure 2.1: Inspiration from tree roots interlocking and modelling the material and interface types leading to an interlocking connection between metals and polymers, which was used for enhancing bonding between Gold and Polydimethylsiloxane(PDMS) [38].

blasting and were able to prove that surface roughness indeed enhances interface strength [42]. Similarly, chemical etching [43], [44], laser treatment [45] and plasma electrolytic oxidation [46] on metal surfaces resulted in a porous structure, which when bonded with polymer provided for a large contact area between them and favours interlocking.

Friction stir spot welding to improve Al and polymer joints was performed with a modified approach involving drilling holes into the Al plate and having molten polymer poured during the welding procedure [47]. The studies conducted by Paidar [48], Pabandi [49], and Aliasghari [46] effectively explored this topic. Aliasghari et al. [46] found that the infiltration of polymer into these holes resulted in mechanical keying, which contributed to the enhancement of joint strength.

Likewise, interlocking can be classified into occurring at multiple scales based on the types of features involved. In the above experiments, Injection Moulding Direct Joining (IMDJ) and micro-geometries through sandblasting can be considered to be interlocks occurring at the micro level whereas chemical treating and etching, at both the micro and nano levels through the presence of pores. Polymer infiltration and keying within metallic plates can be considered as interlocks occurring on the macro scale.

Injection Molded Direct Joining (IMDJ) is utilized amongst metal and polymer to achieve a micro-scale interlocking [50], [44], [51], [52]. Metal surface is treated to form micro and nanostructures, upon which molten polymer is injected onto. The polymer flows into these irregularities and solidifies, upon which the metal-polymer joint is achieved by interlocks as seen in Figure 2.2. Deeper infiltration of polymer and tighter contact resulted in reduced stress concentrations and a higher joining strength between the two.

Macro scale interlocking structures are considered to be the easiest to fabricate using advanced manufacturing methods [37]. It is already used extensively to promote connection in stretchable electronics. The potential to design and directly implement interlocking structures through 3D printing processes already exists. Interlocks at the micro and nano levels require specially fabricated procedures to avoid damage to small-scale structures. Thus, mechanical interlocking requires precise manufacturing methods involving 3D micro/nano printing and 3D lithography to facilitate interlocking during the fabrication of components [37].

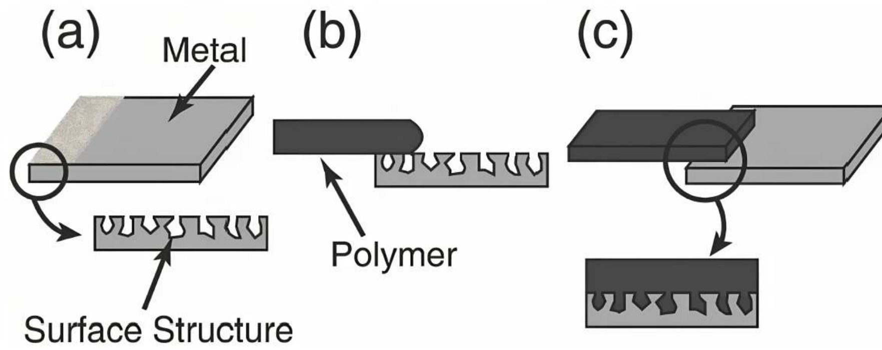

Figure 2.2: Schematic of IMDJ process. This depicts the micro and nano structures on the metal surface followed by application of molten polymer in dark grey. After the polymer solidifies, formation of metal-polymer interlocks are observed [50].

2.4 Previous work by Neuvel

Towards identifying and developing a reliable form to secure conductors to 3D printed conducting structures, in [12] a variety of joint contact setups were tested to study the potency of mechanical adhesion while ensuring electrical conduction.

As part of the exploratory research, Palmga Innovation engineered thermoplastic polyurethane (PI-ETPU) and Proto Pasta conductive polylactic acid (PLA) were selected as conductive polymers, along with thin copper tape as a conductor. Engineering thermoplastic polyurethane (ETPU) is rubber-like, which makes it suitable for flexible applications when compared to electrically conductive composite polylactic acid(EPLA) [53] which is comparatively rigid. The copper tape was placed on a non-conductive base and the conductive polymer was affixed to the tape. Tape surfaces were subject to treatments across individual samples and then had the conductive polymer printed over. A necessary requirement was to ensure that the conductive polymer is physically spread over the copper tape to produce maximum contact to ensure a reliable electrical connection. The polymer is then pulled apart to gauge the mechanical adhesion to the copper tape [12].

The results showed that polymer tracks printed over perforated copper tape remained the only sample able to withstand a simple pulling force. The polymer extruded through the holes fused seamlessly with an underlying non-conductive base polymer (See Figure 2.3). The fused polymer is observed to be intact even when the copper tape was peeled off as seen in Figure 2.4 [12].

Figure 2.3: A cross sectional view of a sample with EPLA extruded over perforated copper tape on a base layer of PLA. The green circles indicate where polymer has successfully penetrated through the holes and bonded with the base layer [12].

A successful fusion occurred at a defined optimal print bed and nozzle temperature. This is theorized to occur as lower environmental temperatures would cause quicker polymer cooling to occur thereby preventing the molten polymer from flowing through the holes to fuse with the base layer.

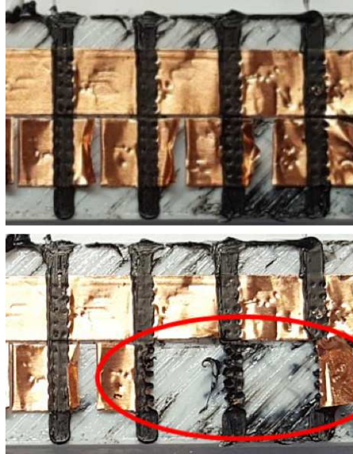

Figure 2.4: Tracks of ETPU printed on a pair of perforated copper tapes which are mounted on a base layer of TPU (NinjaFlex) [54] with a bed temperature of 60 °C to 65 °C (top). The red circle depicts the ETPU having fused with the base layer through the copper tape. These polymeric stakes are formed as they penetrate through the perforations in the copper tape and are observed here when the tape is pulled away (bottom) [12].

Printing polymer over perforated copper tape is seemingly the best candidate for mechanical adhesion between dissimilar materials like metal and conductive polymer, whose underlying mechanism is classified as mechanical interlocking.

2.5 Conclusion

The exploration of adhesion mechanisms reveals the limitations of traditional bonding methods with regards to connecting metals and polymers. Understanding the events occurring at the interface along with the role of surface morphology and contact resistance, provides insights into the complexities involved in achieving reliable adhesion. Chemical bonding and physical adsorption are often insufficient due to the diverse properties of these materials. However, mechanical interlocking emerges as a promising solution.

Mechanical interlocking, with its ability to enlarge the contact area and create interlocks at various scales, offers a unique solution, addressing low mechanical strength and extensive surface preparation. The review of metal-polymer adhesion emphasize the complimentary properties of these materials and the need for standardising a joining method. While adhesive techniques and welding face limitations, mechanical interlocking occurring at the macro, micro and nano scales proves to be a versatile method.

The previous work presented in this context, particularly the experiments connecting conductors and 3D-printed polymers, demonstrates the feasibility and potential of mechanical interlocking. The successful fusion of polymers with perforated copper tape highlights the importance of precise printing parameters for optimal results.

The next chapter will set the stage for the mechanical interlocking with regards to the choices made, sample designing and studying the contact resistance in depth.

3 Design And Modelling

In this chapter, an overview of the design choices required to fabricate a mechanically interlocked metal-polymer sample is given, followed by a discussion of part of an experimental setup model best suited to quantify the simultaneous electrical and mechanical performance of the sample. A lumped model of the sample is utilized to understand how to better measure the contact resistance which also includes modification of the sample into having 4 contacts. Analysis of the undesirable constituent assists in further optimizing the sample to aid in measurement.

3.1 Design Requirements

An individual sample comprises the conductive polymer and metallic conductor, both of whose design choices have implementation challenges that need to be taken into consideration. One of the first considerations involves the fabrication being FDM process compatible. This would involve thermoplastics in filament form undergoing expansion, while being extruded through a nozzle, and selectively deposited layer by layer. This requires a 3D CAD model of the design and knowledge of the properties of the chosen material for printing.

Considering the necessity of quantifying the performance, there is a need for having access to multiple samples having similar properties. It would be worth having access to smaller samples for faster printing times but also allowing for multiple samples produced in a single iteration.

Achieving good contact between the polymer and conductor is to be considered electrically and mechanically:

- Low electrical resistance at the region of contact between conductor and polymer. This will be considered as contact resistance.
- A robust structure that combines flexibility and conductivity.
- Mechanically robust to withstand bending, tensile/compressive deformations and damage due to fatigue
- Simple fabrication process with freedom for customization for corresponding applications

As the design progresses, it is essential to accommodate features that will make it suitable for testing as part of an experimental test setup.

3.1.1 Polymer

Based on the research and experimentation by Patrick Neuvel [12], perforated copper tapes achieved the best form of mechanical interlocking with polymer printed over it. This provides a foundation regarding the choice of material and the type of mechanical adhesion. ETPU was chosen for fabrication, testing and any future recommendations due to its flexible nature. It had lower resistivity when compared to Proto Pasta [55]. Requirements for the fabrication of samples will be considered in detail in Chapter 4.

3.1.2 Conductor - Copper wires

Copper wires are extensively used as part of electrical circuits for their conductivity, coupled with their ease of use and availability. Generally, the thin and flexible nature could allow for intricate routes and compact designs. Achieving mechanical interlocking using copper wire and polymer could occur on a macro scale level as discussed before.

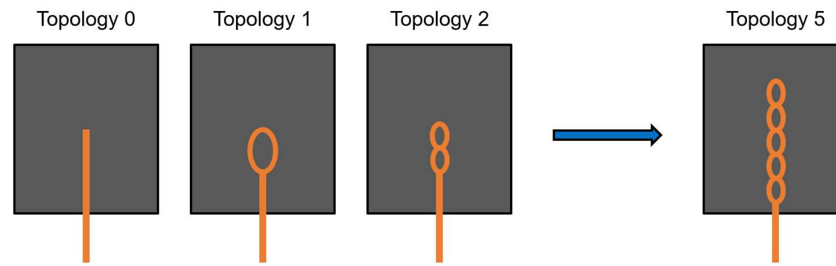

Figure 3.1: A depiction of various geometries for embedding of copper wire in polymer, as seen from a top view, and nomenclature of topology. With topologies of 1 and higher, there is always enclosed area of polymer to pass through one or more loops.

The level of interlocking will depend on the geometry used but also the topology of the copper wire which will be secured within the polymer. In this case, topology can be defined as the physical arrangement of the wire with labels given to increment with the number of loops(See Figure 3.1). A closed loop will allow for the polymer to pass through and physically interlock with the wire. Increasing the number of interlocks will increase the overall strength of the connection.

Copper wire embedded inside polymer

As experimented by Patrick Neuvel, it is interesting to consider copper wires with regards to the additive manufacturing technique used, namely FDM. This can provide insight into the optimal choice of conductor geometry of the perforated tapes and wires.

An ETPU block was printed and copper wire is placed, after which more layers of polymer were printed. This experiment was performed to check how well copper wire behaves similar to the sample fabrication method as performed by Patrick [12].

A mismatch between the radius of the wire and the groove within the polymer matrix caused the wire to slide out. This is also attributed to the minimum print resolution of the nozzle. Replacing a single strand with a multicore wire, it was observed that there was potential misalignment produced due to collisions with the printing nozzle. These collisions also led to some strands being isolated away from the rest (See 3.2).

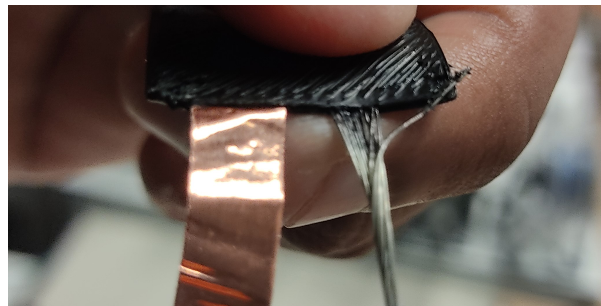

Figure 3.2: A flexible polymer block with copper tape and multicore wire embedded. One of the wire strand has been displaced physically from the rest by the motion of the printer nozzle.

Observations

Ensuring the precise alignment and positioning of wires within the 3D printed structure demands meticulous attention and is poorly controllable in this method. Any misalignment dur-

ing the layer-by-layer printing process can lead to misconnects or incomplete electrical paths. Twisting of wires and loosening creates complications towards producing uniform samples which needs to be studied. It is also important to mention the additional complexity involved in placing these wires with high level of coordination and precision onto the block of polymer, only for collisions with the nozzle to cause disorientation.

Consistent adhesion was clearly lacking between the wires and the polymer material. Contact surface area between the polymer and wires can also be considered to be small. The wires could be pulled away from the polymer bulk which indicated that there was no form of interlocking, to withstand a pulling force, present.

3.1.3 Conductor - Perforated Copper tape

Copper tape inevitably emerges as the superior choice over copper wires within the realm of FDM printed electronics, drawing from the insights obtained from Patrick's research [12]. In contrast to the limitations experienced by utilizing copper wires, perforated copper tapes offer a transformative solution.

Acrylic-backed perforated copper tapes, as used by Patrick, can be considered as a fixed geometry, eliminating misalignment concerns. While the acrylic glue does not assist in securing the tape onto the polymer, due to incompatibility, controlled heating with a soldering rod to secure polymer stakes through the holes mechanically interlocks and secures the tape. The tape is also thin and flexible, and its flat surface allows it to conform with additional polymer layers extruded on top and to adapt to mechanical stresses.

Properties

A thin flexible copper tape with holes helps in minimizing stress concentrations when compared to a solid conductor without any perforations [15, 56]. The stress concentration factor (SCF) of a structure is influenced by it's shape and thickness and is defined as the ratio of the maximum stress in the material to the nominal stress applied [56]. A thin material has lower SCF than a thicker one and a flexible material has a lower SCF than a rigid material. Accordingly, a material with holes has a lower SCF than an inlay without since the holes act as stress relievers. The number of perforations on the tape (see Figure 3.3 can influence the degree of interlocking and overall strength of the connections. More holes may accommodate more molten polymer for better interlocking but it is necessary to also think about how this can simultaneously weaken the tape's overall structural integrity during pulling.

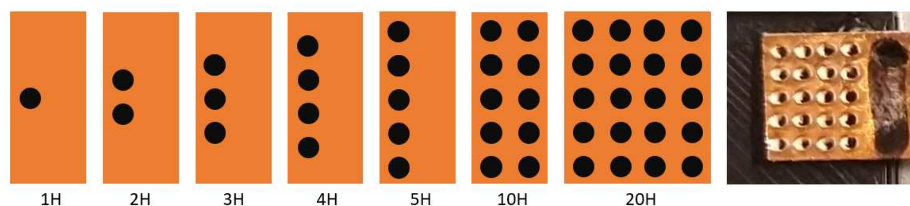

Figure 3.3: Schematic of potential patterns for increasing the number of holes in various tapes. The label below every sample indicates the number of holes to be perforated. The photo on the right depicts a copper tape with 20 holes resting on a piece of ETPU.

The shape of the holes in the tape could also influence interlocking. While irregular or complex shapes may enhance interlocking when compared to simple shapes like circles, their fabrication would involve laser cutters or any potentially automated complex processes. Sharp corners of the tape within complex shaped holes in contact with polymer could incur wounds, stress concentrations or mechanical weakening [15,56]. Achieving consistent results with com-

plex shapes may be more challenging due to a large number of samples required for testing, where a slight variation in hole geometry can impact performance. Circular holes were chosen and perforated into tapes using the same jig used by Patrick in Phase II [12].

The orientation or pattern of the holes can also impact the potency and stability of the interlocks formed. Spacing and distribution of holes across the tape can determine how evenly stress is distributed during mechanical loading. Two common patterns to be considered are ortholinear and staggered as seen in 3.4.

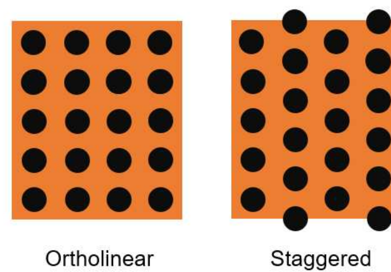

Figure 3.4: Schematic of Ortholinear and Staggered hole patterns on a copper tape.

A staggered hole arrangement can provide better stress distribution across the entire pattern, reducing the risk of localized stress concentrations. However, an ortholinear pattern of perforations is chosen for uniform mechanical interlocking and its simplicity in design and fabrication. Aiding to this is the immediate availability of the punching jig with ortholinear pattern [12] (See Chapter 4 for more details) used by Patrick. A staggered hole pattern can be implemented in the future to comparatively check for improvements based on the results provided by the ortholinear hole pattern.

3.2 Basic Sample

Based on the considerations a basic prototype sample is designed, keeping an overall simple process, minimizing material consumption along with the necessity for fabricating duplicates for testing. A basic CAD model can help to visually understand the design for any further changes as necessary (See Figure 3.5). This sample is named "2 tape sample" for reference.

Copper tapes are perforated prior to printing an even layered block of polymer. The printing is commanded to pause upon extrusion of half the total number of layers. This is where the copper tapes are secured after which the remaining half of the layers is extruded over the tapes. This produces a complete copper-ETPU mechanically interlocked sample (See Figure 3.6). Keeping the print bed dimensions in mind, further considerations can be done to be able to produce multiple samples at once.

Samples are sliced through their cross section to observe the interlocks at the macro level. This gives insight regarding the nature of the contact. Tapes are pulled away from the polymer block

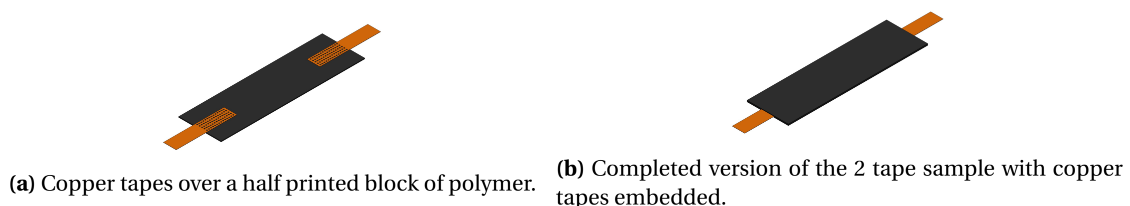

(a) Copper tapes over a half printed block of polymer.

(b) Completed version of the 2 tape sample with copper tapes embedded.

Figure 3.5: CAD model depicting the 2 stages of fabrication to produce a 2 tape sample.

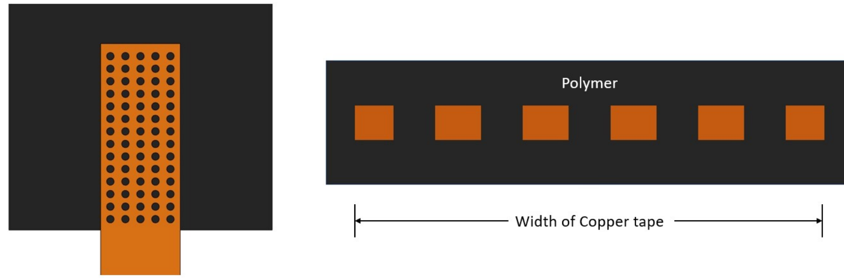

Figure 3.6: Schematic depicting the hole pattern on the copper tape embedded within the polymer along with a cross sectional view. The polymer filled region between the blocks of copper represent the stakes that occur when polymer flows through perforation.

in a controlled manner to enable to identify the breaking point, and the number of load cycles it can withstand as function of the various parameters as discussed above.

3.3 Modelling

Contact resistance represents the electrical resistance at the interface between electrical contacts and is a part of the total resistance of the system [57]. In the sample, contact resistance arises due to the unpredictable conduction between the tape and polymer, being influenced by contact area, surface roughness, individual material properties, tightness of contacts and the mechanical integrity of the interlocks. Specifically, this interface would classify as the point where the perforated copper tape and polymer (PI-ETPU) come into contact and interlock. This region has been pictorially represented in the cross sectional view in Figure 3.6. Contact resistance embodies a primal aspect of electrical performance evaluation, specially when considering a flexible and conductive 3D printed structure. Quantifying contact resistance serves as a bridge between the mechanical and electrical domains, providing an insight about how mechanical interlocking between perforated copper tape and ETPU influences electrical conduction. Currently explored and employed methods for measuring contact resistance are 4-point sensing [58] and the Transfer Length Method (TLM) [59]. These methods can be complex to implement when we consider measuring electrical performances of flexible samples simultaneously under mechanical loading.

Contact resistance is essentially an impedance to the path of current flow due to the insufficient electrical contact and hence can be a source of heating through the Joule-Lenz effect [60, 61]. Heating of contact surfaces is thereby one of the more adverse effects of contact resistances. Increase in contact resistance has also been commonly attributed to fretting corrosion [62] and looseness of contacts. The former occurs by wear and tear of contacts which are subjected to micromotion due to temperature variatioins or vibrations. Research has indicated that an increase in contact resistance is mainly attributed to relative motion between electrical contacts [63]. Admittedly, the electric contacts within the sample are hidden in the bulk of the polymer matrix, which obviously brings challenges to obtain the response of physical parameters such as quality of mechanical interlocks and the copper-polymer interface without destructive testing. Currently, research about the effect of bonding methods on the contact resistance are very limited [8–10]. Thus, contact resistance is a way to obtain insight about the quality of electrical connections while also ensuring less impedance to the path of current. Modelling a setup required to perform tensile and electrical measurements simultaneously could depict the robustness of the interlocked contacts.

3.3.1 2-wire resistance measurement

In the context of our research, a practical 2 wire connection is considered with the designed 2 tape sample whose resistance R is to be measured (See Figure 3.7. All wire and test leads have some resistances, which are denoted by R_w respectively on both wires connecting the contacts of the sample [64, 65]. In this situation, the resistance meter would now measure the resistance which includes the combination of wire resistances and the sample resistance R.

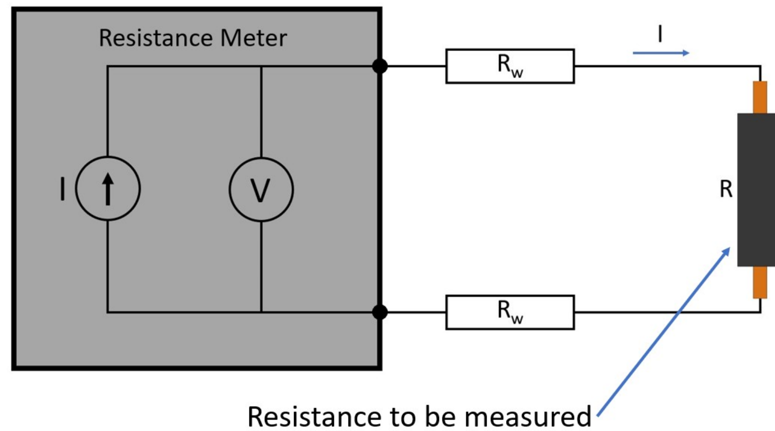

Figure 3.7: 2 wire resistance measurement circuit.

The resistance meter yields:

$$R_{\text{2-wire}} := R_\text{w} + R + R_\text{w} \tag{3.1}$$

Despite only desiring the value of R, there are additional resistances adding to the 2 wire resistance measurement which are dependant on the wires. These can not be eliminated regardless of the quality of the wires. The contact resistance also only accounts for a small fraction of the total resistance and this method is also limited in its ability to differentiate between the contact resistance and the sample's bulk resistance. This is also an unexplored limitation of the sample design having only a single path for the current to flow [64, 65].

3.3.2 3-wire and 4-wire resistance measurement

In a 3-wire resistance measurement, a separate wire is utilized to measure the voltage drop over the sample whose resistance R is being measured. Consider a practical 3-wire resistance measurement as seen in Figure 3.8. The lower half of the connection is similar to the 2 wire connection, maintaining a single wire as path for the measurement current and for the voltage measurement. The voltage measurement wire in the top half is again connected to the resistance to be measured, however the resistance R_{w2} in this wire does not influence the voltage measurement. Due to the high internal impedance of the voltage meter, there is a very negligible amount of current flowing through this wire, which generally be ignored for all practical purposes. So, presence of resistance R_{w2} in this wire does not cause any voltage drop. The resistance meter can compensate for the top wire resistance however the lower half has no means to compensate for the resistance R_{w3} [64, 65].

The resistance meter yields:

$$R_{\text{3-wire}} := R + R_{\text{w3}} \tag{3.2}$$

It is observed that resistance R_{w1} is eliminated from the measurement. It is still better than 2 wire measurement.

In a 4-wire resistance measurement, 2 separate wires are utilized to measure the voltage drop across the sample whose resistance is being measured. Consider a practical 4-wire resistance

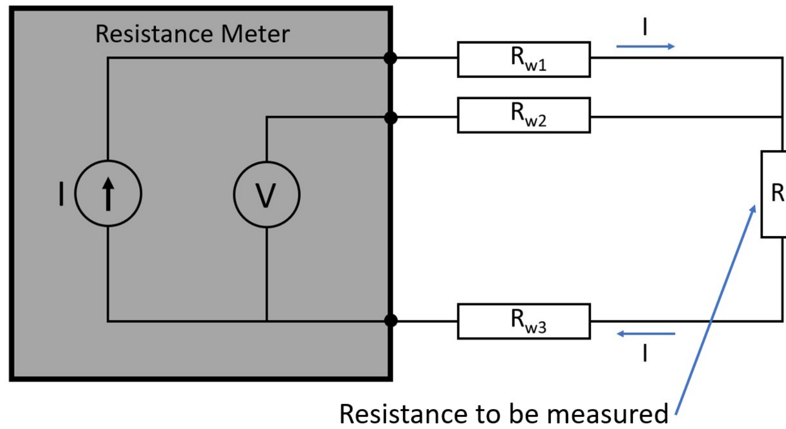

Figure 3.8: 3-wire resistance measurement circuit.

measurement as seen in Figure 3.9. The wires measuring voltage across the sample are classi-

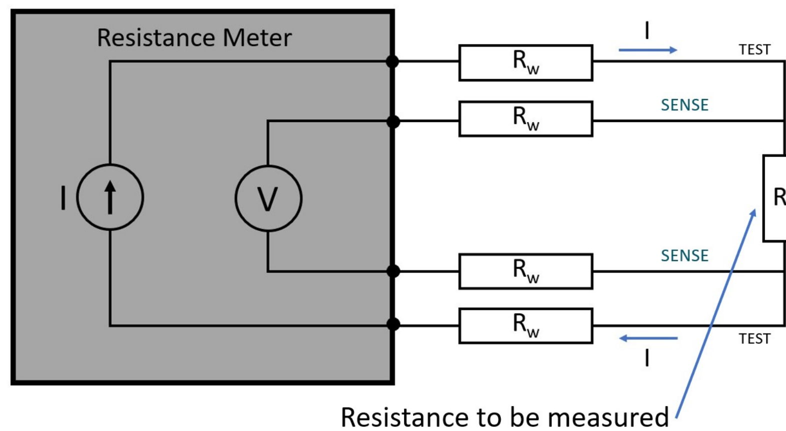

Figure 3.9: 4-wire resistance measurement circuit.

fied as Sense leads which are connected to the ends of the resistance to be measured. Current passes through the outer wires which are classified as Test leads. Once again, there is negligible amount of current flowing through the sense leads so presence of wire resistances on the sense leads does not cause any voltage drop, thus eliminating any errors. Hence, voltmeter measurement is essentially the same as the voltage across resistance R.

Hence, the resistance measured here is:

$$R_{4\text{-wire}} := \frac{V}{I} = R \tag{3.3}$$

As a result, the sample resistance value can be measured more accurately than both 2 and 3-wire measurement methods. The sensing leads must be connected as close to the resistance R as possible [64, 65], so that it excludes the resistance from any part of the testing leads.

Using a 2 tape sample in place of the resistance to be measured would provide us with the total resistance of the entire sample and wires. Contact resistance is more specific to the interface, occurring between individual perforated copper tape and the ETPU interlocked with it. This means that there is no way to isolate the contact resistances of the tapes from the ETPU bulk

resistance. This demands a change in the sample design such that, the difference between the 3 and 4-wire resistance measurement can isolate the contact resistance of a specific tape while the tape experiences a pulling force.

3.3.3 Characterization

The separation of the sense and test leads in the 4-wire measurement method, necessitates 4 connections. The sample requires 4 contacts in order to utilize the method. Consider a new mechanically interlocked sample with 4 copper tapes as shown in Figure 3.10.

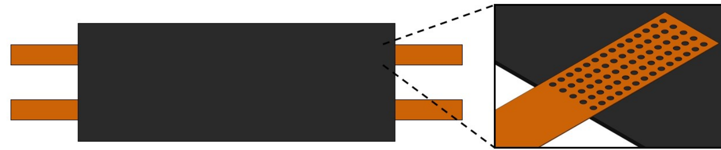

Figure 3.10: Schematic of an ETPU sample with 4 copper tapes mechanically interlocked within. A zoomed in view depicts the perforations on each tape embedded within.

A lumped model of this sample is presented in Figure 3.11 which provides a better understanding of the constituents onboard. Contact resistances are indicated by orange contacts, the bulk resistance of the ETPU sample is represented by the two blue $2R_\mathrm{b}$ resistances. A parasitic resistance termed as R_3D occurs between 2 adjacent tapes. Any current that passes between two proximal contacts across the plane encounters this resistance. The individual resistances of the copper tapes themselves are insignificant and are not considered in the lumped model.

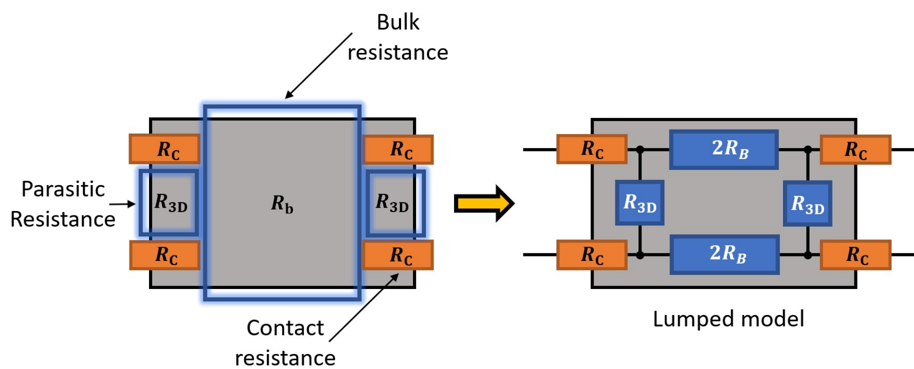

Figure 3.11: Schematic representation of the physical structure (left) of the 4 tape sample along with its constituent resistances and a lumped model (right) expressing the same in terms of corresponding resistors and connectors.

3.3.4 Difference in 3-wire and 4-wire resistance modelling

This lumped model (Figure 3.11) can now be considered onboard 3-wire and 4-wire resistance measurement circuits.

In the 4-wire configuration (See Figure 3.12), no current passes through the top contacts, hence the values of R_C are not considered here. However, current passing through the top part of the bulk resistance (I_2Rb) is of importance. The model equation for the 4-wire resistance R_4 measurement based on the 4 tape sample yields:

$$R_4 := \frac{V_1 - V_2}{I_\mathrm{in}} = \frac{(2R_\mathrm{b})(I_\mathrm{2Rb})}{I_\mathrm{in}} = \frac{(2R_\mathrm{b})(2R_\mathrm{b})(I_\mathrm{in})}{(I_\mathrm{in})(2R_\mathrm{b} + 2R_\mathrm{b} + 2R_\mathrm{3D})} \tag{3.4}$$

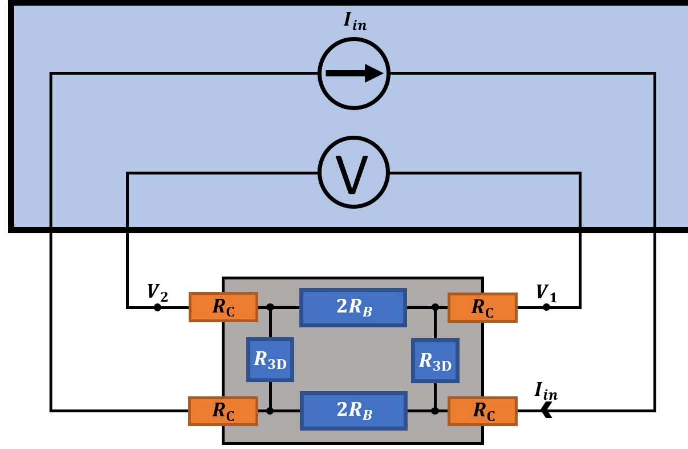

Figure 3.12: Schematic of the lumped model of the 4 tape sample incorporated into the 4-wire resistance measurement circuit to determine the contact resistance of the top right electrode. The input current I_{in} flows through the bottom contacts while the voltage is measured over the top contacts.

$$R_4 = \frac{R_\text{b}}{1 + (R_{3\text{D}}/2R_\text{b})} \tag{3.5}$$

No contact resistances are considered in the above equation, as in the 4-wire resistance method, almost no current passes through the contacts. $V_{\text{input}}/I_{\text{in}}$ is the measured resistance of the system which is essentially $2R_\text{b}$ resistance at the top lying in parallel with the remaining resistance elements.

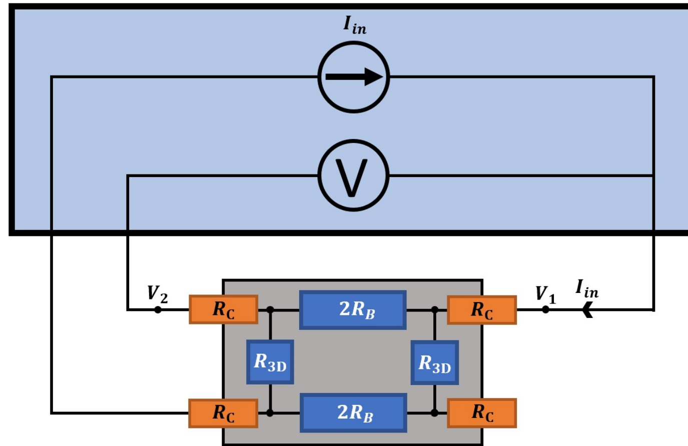

Figure 3.13: Schematic of the lumped model of the 4 tape sample incorporated into the 3-wire resistance measurement circuit to determine the contact resistance of the top right electrode. The input current I_{in} flows through the top right contact and exits through the bottom left contact. The voltage is again measured over the top contacts.

In the 3-wire configuration, see Figure 3.13, the input current passes through the top left contact, which will be considered here. Similar to the 4-wire measurement, current passing through the top part of the bulk resistance ($I_{2\text{Rb}}$) is of importance. The model equation for the 3-wire resistance R_3 measurement yields:

$$R_3 := \frac{V_1 - V_2}{I_\text{in}} = R_\text{C} + \frac{(2R_\text{b})(I_{2R_\text{b}})}{I_\text{in}} = R_\text{C} + \frac{(2R_\text{b})(2R_\text{b} + R_{3\text{D}})(I_\text{in})}{(I_\text{in})(2)(2R_\text{b} + R_{3\text{D}})} \tag{3.6}$$

$$R_3 = R_C + R_b \tag{3.7}$$

The tape at the top right is the one whose contact resistance is under study. The difference between the model equations for the 3-wire resistance R_3 and 4-wire resistance R_4 yields:

$$\Delta R_{3,4} = R_3 - R_4 = R_C + R_b - \frac{R_b}{1 + (R_{3D}/2R_b)} = R_C + \frac{R_{3D}}{2 + (R_{3D}/R_b)} \tag{3.8}$$

An assumption is considered that the bulk resistance R_b is considerably greater than parasitic resistance R_{3D}, thus $\frac{R_{3D}}{R_b}$ is negligible.

$$\Delta R_{3,4} \approx R_C + R_{3D}/2 \tag{3.9}$$

It is observed that the measurements yield the contact resistance and an additional term $R_{3D}/2$ due to the interplanar offset of electrodes from one another. Contact resistance of a specific contact could change if external force is applied exclusively. This sample could be fixed on a testing setup for a near simultaneous 3-wire and 4-wire resistance measurements to be performed with a pulling force on a contact to observe the behavior of the contact resistance.

Dependencies on Parasitic Resistance

The value of the contact resistance R_C is the unique objective from the measurements and from Equation 3.9. It is measurable only when $R_C > R_{3D}/2$. The parasitic resistance R_{3D} is solely contributed and affected by the inherent geometry in the polymeric region between the samples.

Here, it is very important to define labelling terminology utilized before proceeding further.

Contact resistivity (henceforth considered as σ_C) is labelled as a surface property arising from the contribution of the true contacting areas of copper and ETPU at the interface.

Parasitic resistivity (henceforth considered as ρ_{3D}) is labelled as a material property that is clearly dependent on its own intrinsic features. Here, the term is defined by the ETPU's unique molecular structure, as the parasitic element is classified for being within the ETPU region between adjacent copper tapes (See Figure 3.11).

Considering this, change in $\Delta R_{3,4}$ is linear with both contact resistivity and parasitic resistivity. R_{3D} can be thus minimized by making specific geometrical choices for the sample. A schematic depiction of the interior region between the tapes is seen in Figure 3.14. In this scenario, a 2 dimensional approach is considered where current direction is assumed to be moving from the copper tape into the bulk and the proximal region in the same plane. Further research is required to model the exact direction of currents in the 3 dimensional aspect as this plane is in fact sandwiched by more layers of ETPU all around.

$$R_C > R_{3D} \tag{3.10}$$

$$\frac{\sigma_C}{A_C} > \frac{\rho_{3D} L_{3D}}{A_{3D}} \tag{3.11}$$

From Figure 3.14 and Equation 3.11, it can is inferred that parasitic resistance R_{3D} can be minimized by reducing the length or rather, the distance(L_{3D}) between adjacent copper tapes. Similarly, increasing the cross sectional area A_{3D} reduces R_{3D}. To reduce the 3D deformation happening between the region of adjacent copper tapes during pulling, the entire sample's width can also be reduced. Both of these design choices can be physically implemented during the fabrication process up to a certain degree. These are clearly discussed and incorporated in the next section.

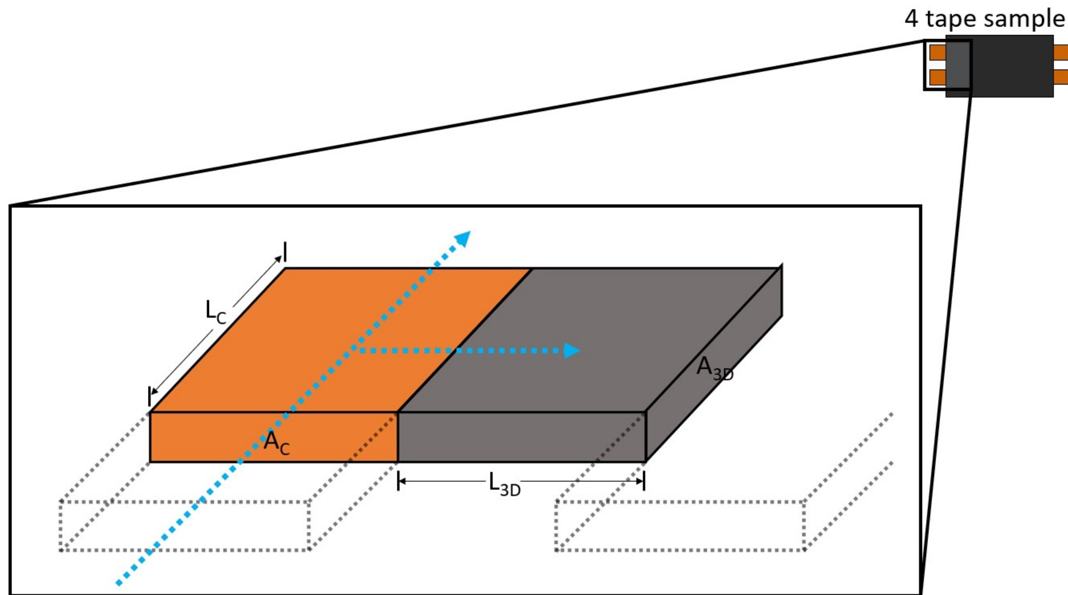

Figure 3.14: Zoomed in view of the 4 tape sample depicting the interior region where adjacent copper tapes are embedded. The blue dotted arrows indicate the assumed directions of current strictly within the plane. Embedded copper tape contributes to the contact resistance whereas the polymeric bulk contributes to the parasitic resistance. A indicates their respective cross sectional area perpendicular to the direction of the current whereas L indicates their respective length.

3.4 Revised Sample Design

The main prospects to consider from the modelling involve:

- Using 4 copper tapes as contacts for a 4 tape sample.
- Reducing the gap between two adjacent copper tapes. This would also be dependant on the minimum print resolution of the 3D printer nozzle.
- Reducing the sample width to reduce the 3D deformations.
- Considering a hole on the sample for securing a bolt through it, in order to mount on the experimental setup for being stationary when the copper tape is pulled.

Recapping other general considerations

- Minimal size in order to fabricate multiple samples at one iteration. This would also require considering the size of the print bed and time taken for individual sample fabrication.
- Even number of layers, so as to pause and mount copper tape in the middle.

These considerations are detailed with their dimensions and presented in the next chapter.

3.5 Conclusion

The design of the sample is optimized by analyzing the lumped model and its undesirable constituent (R_{3D}). This design can now be modelled in an appropriate CAD software and fabricated. This can finally be utilized onboard an experimental test setup where the 3-wire and 4-wire measurements are done simultaneously as one of the copper tapes is influenced by an external force.

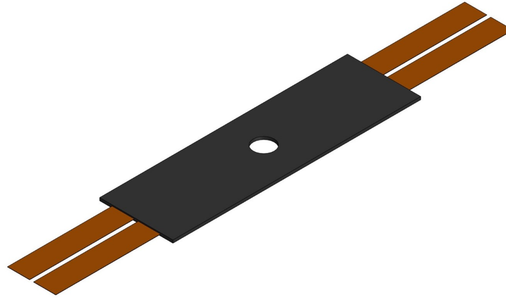

Figure 3.15: CAD design of a revised sample design with the changes incorporated.

The next chapter details the materials used and fabrication process required to create a mechanically interlocked copper tape - ETPU sample.

4 Materials and Fabrication

4.1 Introduction

In this chapter we delve into the crucial aspects of materials selection and fabrication procedures undertaken to create test specimens for a comprehensive study on the mechanical and electrical performances of mechanically interlocked metal-polymer hybrid materials. It focuses on the integration of copper tape and a conductive polymer, specifically PI-ETPU 85-700+, to form mechanically interlocked structures. Additionally, this chapter outlines the 3D models, electric contacts, 3D printers and polymers utilized in the experimental setup, providing a foundation for subsequent analyses. In later sections the specific materials used, the printing parameters and the technique employed to ensure a consistent and controlled manufacturing process will be detailed. This chapter is concluded by presenting the final samples after fabrication, setting the stage for exploration of their mechanical and electrical behaviors in the experimental setup discussed in the following chapter.

4.2 Materials and Equipment

4.2.1 Electrical Contacts

The electric contacts are comprised of 6.35 mm wide and 66 µm thick copper tape (See Figure 4.1) with a conductive acrylic adhesive on one side [66].

Figure 4.1: 3M Copper tape with adhesive backing . [66].

4.2.2 Polymers

(Palmiga Innovations) PI-ETPU 85-700+ conductive flexible filament

This 3D printing filament is both flexible and conductive, having been manufactured from thermoplastic polyurethane. This was an unreleased filament from Palmiga Innovations, whose conductivity before printing is 80 Ω cm [55]. The maximum extension as reported by the manufacturer is more than 700 % [67].

(Ultimaker) ToughPLA

This a non conductive polylactic acid material that is optimized for fabricating tough parts like tools and jigs. Primarily used for fabricating clamps, assistance tool and base platform required for experiments. These tools are further detailed in the next chapter.

[68]

4.2.3 Printers

Diabase H-Series 3D printer.

This multi-material printer is capable of printing with up to 5 filaments, which are switched or chosen based on a turret configuration (See Figure 4.2). This printer is primarily used to fabricate the conductive polymer block and an assistance tool for connecting the copper tape to the polymer block.

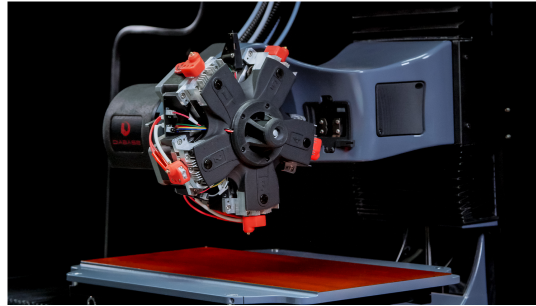

Figure 4.2: Diabase H-Series Multi-Material 3D printer.

Ultimaker S3 3D printer

This printer [69] fabricates the essential non-conductive parts required for the experimental setup.

Associated printing software

- Dassault Solidworks 2021, as CAD modelling software
- CURA 4.11, as 3D printing slicer software

4.2.4 Custom punching jig

To fabricate perforations in the copper tape, a custom punching jig (printed by Patrick on a Form 2 stereolithography printer, Formlabs, USA) was utilized [12]. Figure 4.3 depicts the jig and its parts. This jig is complemented by a hand piece consisting of 10, 600 µm diameter hardened steel pins which are trimmed short with edges sanded flat. Upon applying an impulsive force, the pins punch a hole in the tape and displace the copper scrap away from the bulk. A schematic representing this can be seen in Figure 4.4.

The holes are spaced in a rectangular grid consisting of 5, arranged with 1 mm between rows and 1.2 mm between each column. Holes with multiples of 10 can be punched with this jig whereas a single hardened sewing pin is used to punch holes in arrangements of fewer than 10 holes. The top half of the jig's hole layout also gives the flexibility to punch holes in a variety of patterns using a single pin.

4.2.5 Assistance Tool

This mounting aid was developed out of necessity to overcome the challenges of adhering copper tapes to the top of the polymer surface in close contact. There is a constant challenge to reliably attach two adjacent tapes onto the polymer separated by a tiny gap due to the heated bed temperatures and the poor adhesion between the tapes and the polymer itself. It ensures a spacing of 0.8 mm between the tapes. An assistance tool was designed and fabricated as shown in Figure 4.6. It constitutes a marked wing element on which the copper tapes are to be mounted. A handle is utilized as leverage for gripping whereas the dividing notch physically

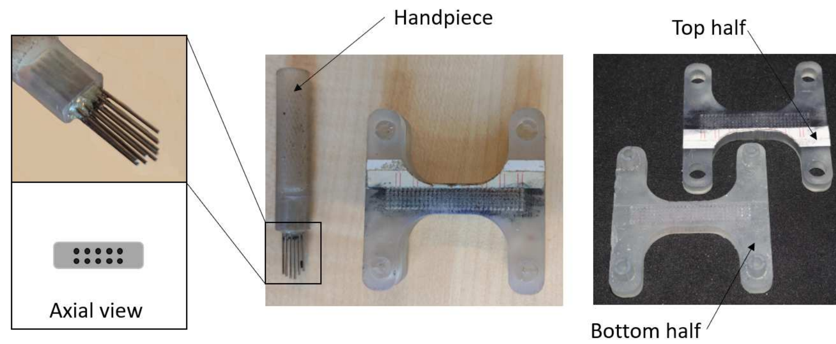

Figure 4.3: Various parts of the punching jig. The jig consists of two halves. The bottom half consists of a groove to house the copper tape securely. The top half clamps fown to ensure a constant alignment of tape thus allowing the user to punch holes [12].

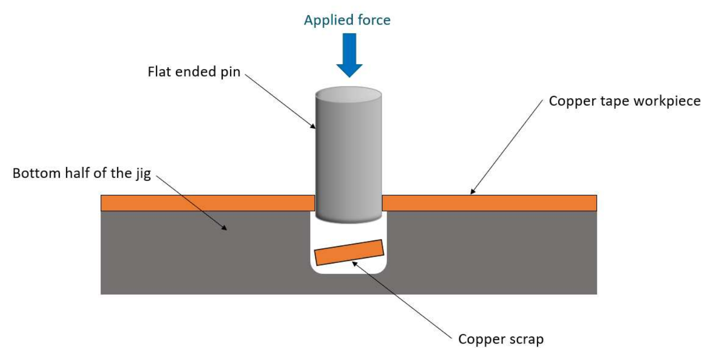

Figure 4.4: Schematic depicting the working of the punching jig.

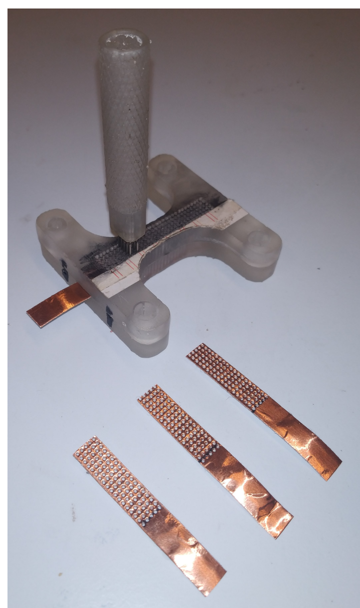

Figure 4.5: The jig securing a piece of copper tape along with the handpiece inserted to perforate the tape. A set of perforated copper tapes are shown beside the jig. [12].

separates the tape when being mounted. It enables a separation distance of 0.8 mm between adjacent copper tapes.

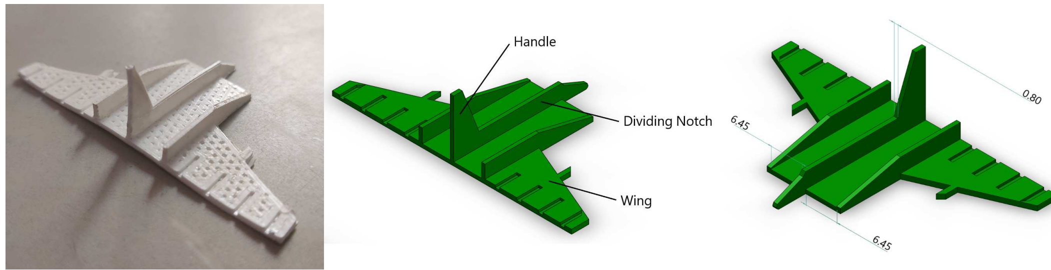

Figure 4.6: Assistance tool along with diagrams of its basic parts and dimensions (mm). This tool is used for mounting the perforated regions of the adjacent copper tapes onto the ETPU block while also protecting the user from the heated bed. The core functionality is to ensure 0.8 mm gap between these tapes. Markers on the wing are used as reference to orient the tool with respect to the polymer matrix.

4.3 Electrical contact fabrication

This section comprises of the detailed steps involved in fabricating the polymer sample, mounting of the perforated copper tape and soldering required to secure the contacts onto the polymer matrix. These are the major steps required in order to complete the mechanically interlocked connection between ETPU and perforated copper tape.

As can be seen in Figure 4.5, holes are punched out of the tape with the help of the specialized punch. The scrap copper is displaced when the flat-ended pins are driven in with enough power to punch a hole. For identification of the respective tapes after the printed polymer encases them, unique markings are input that correspond to the tape's number of holes, the pattern of design and the length of the tape that needs to be encased. These identification markers can be seen in Figure 4.7. Also, samples were made where one copper tape contact is replaced by a frayed multicore wire with an original diameter of 1 mm .

Figure 4.7: A set of tapes with a different number of perforations and identification markers. Shown here from the left are tapes of 20, 0 and 10 holes, with 4.8 mm being the length of the tape to be enclosed by the polymer.

The printed polymer is in the shape of a cuboid of 71 mm x 21 mm x 0.8 mm with a 6 mm hole in the centre, fabricated from PI-ETPU 85-700+ on the Diabase Engineering H series 3D printer. The CAD model utlized is shown in Figure 4.8. Table 4.1 presents the printing parameters utilized while fabricating all samples. As specified, each layer of the polymer sample is 0.1mm amounting to 8 layers.

The nozzle and bed temperatures are set optimally to be high enough to induce seepage of ETPU into the perforations on the copper tape. The extrusion multiplier was initially set to 1 by

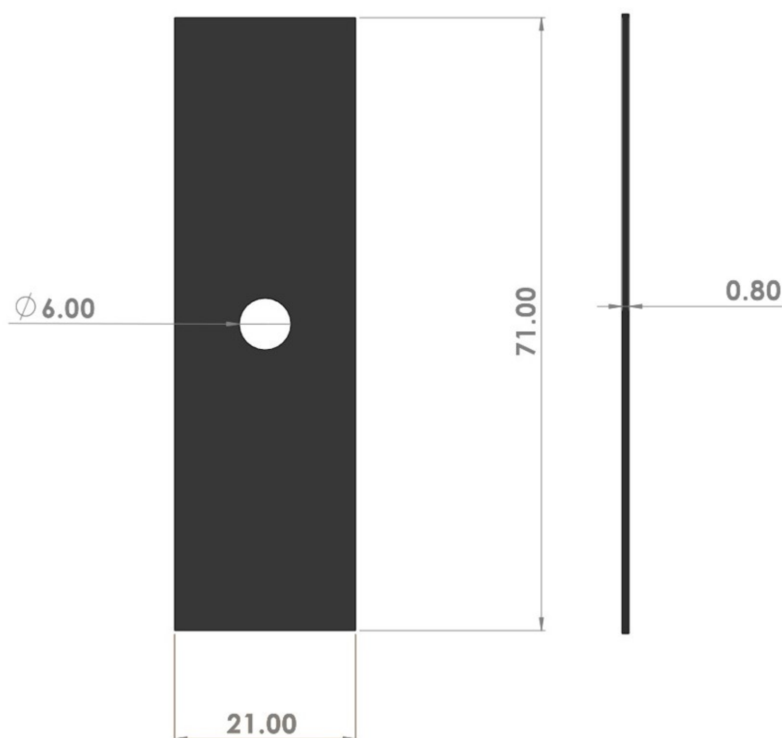

Figure 4.8: CAD Model of the sample's block of ETPU. The dimensions are labelled in millimeter(mm).

Table 4.1: 3D-Printing parameters.

3D-Printing parameter	Value
Bed temperature	65 °C
Nozzle temperature	225 °C
Extrusion width	0.45 mm
Extrusion multiplier	1.3
Infill Density	100%
Infill angle	$+45° \setminus -45°$
Layer height	0.1 mm
Printing speed	$25\,\mathrm{mm\,s^{-1}}$

default, which produced gaps between individual extruded polymer paths. Setting a value of 1.3 eliminated these gaps. A printing speed of $25\,\mathrm{mm\,s^{-1}}$ is considered to be slightly low, so as to give ample time to allow for the extruded molten polymer to seep into the perforation. This defines a good quality interlock. High printing speeds could cause extrusions to skip over small perforations, leading to less effective interlocks.

The printing of the polymer is paused manually when the lower half of the total layers has been extruded onto the heated bed of the printer. With 4 out of the 8 layers extruded, the next step of the fabrication involves the process of mounting the copper tapes onto the polymer before resuming printing, with the objective to encase them.

The copper tapes are mounted onto the assistance tool near the notch beginning from the region where there is no perforation and all the way, to the other end. The markers (See Figure 4.6) on the wings are utilized to align the assistance tool with respect to the half-printed polymer sample, such that both midpoints of the width of the polymer block and wingspan match. With this alignment, the assistance tool is slid toward the polymer block and the perforated re-

gions of the copper tapes are in contact with the polymer matrix. After the tapes are embedded into the polymer, the assistance tool is pulled away manually using the handle as leverage. The notch is primal to ensure a gap all throughout the length of the tape. The non-perforated areas of the tape securely adhere to the printed bed to reduce any potential movements or obstructions to the nozzle when the print is resumed.

The process of mounting perforated copper tapes onto the matrix is better explained through means of Figure 4.9.

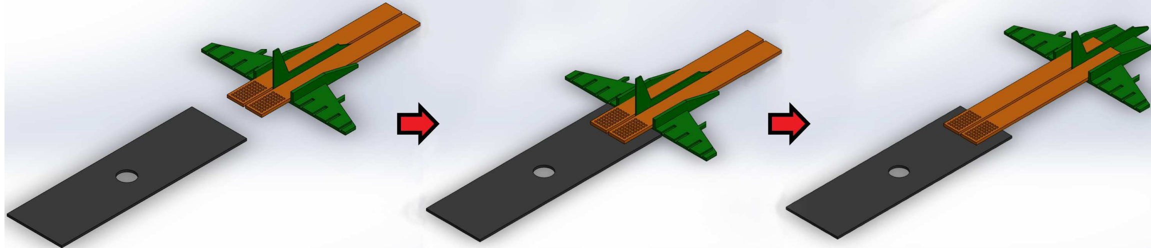

Figure 4.9: Multiple stages of copper tape mounting using the assistance tool. The tool is docked to the polymer matrix, the perforated copper region is held in place and the tool gently removed. This occurs prior to soldering, which completely secures the tape onto the polymer.

Along with copper and polymer being dissimilar materials, the acrylic adhesive on the underside of the tape did not adhere to the polymer surface either. A soldering iron at 350 °C is used to iron the tape on the polymer (See Figure 4.10). Additionally, unidirectional strokes are performed to melt nearby polymer matrix and disperse it towards the edges of the tape. This mechanically fastens the tape onto the sample surface. It was also observed that some of the polymer entered the holes, thereby further assisting in mechanically securing the tape. Figure 4.11 depicts the behaviour of tapes before and after soldering treatment.

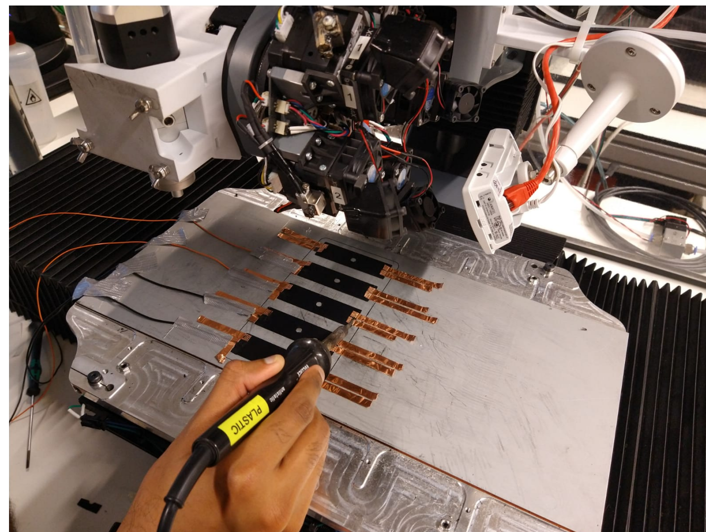

Figure 4.10: Soldering the copper tapes and wires of 5 samples at once. This occurs once half the total layers of ETPU is extruded.

The print is resumed and the remaining layers get extruded over the polymer sample with copper tapes as shown in Figure 4.12. Multiple batches of samples were fabricated in sets of 5 to compensate for the time taken as shown in Figure 4.13.

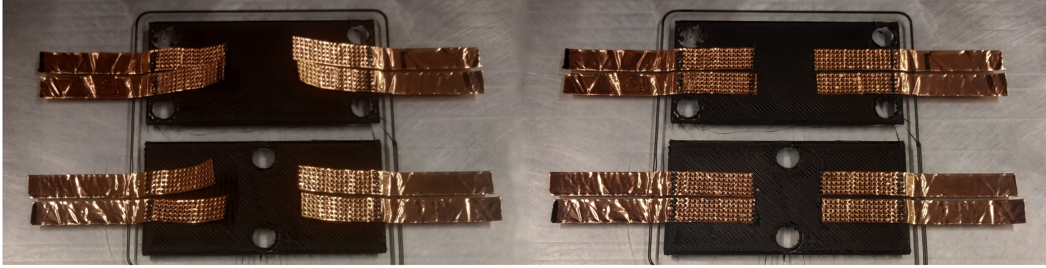

Figure 4.11: Copper tapes before soldering (left) do not adhere flat on the polymer surface even with acrylic glue backing. After soldering (right), the tapes are securely placed within the polymer matrix.

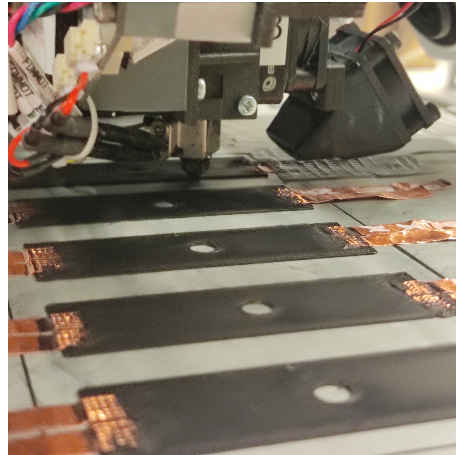

Figure 4.12: Resuming printing on polymer samples after the copper tapes have been mounted and soldered.

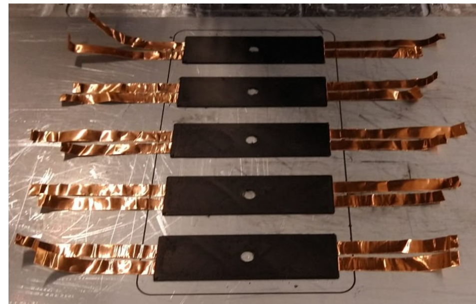

Figure 4.13: A set of 5 samples after fabrication on the heated printing bed.

4.4 Final samples

Samples can be differentiated based on the physical shape of the conductor, namely tape and wire. Tape samples can further be distinguished by the number of holes perforated onto them. Wire samples are essentially multi-core frayed apart and basically undergo the same procedure as mounting of tapes mentioned in the previous section. Figure 4.14 depicts the two types of samples fabricated.

This intricate sample consisting of mechanical interlocks are sliced across the cross section for observation. These results are discussed in Chapter 6.

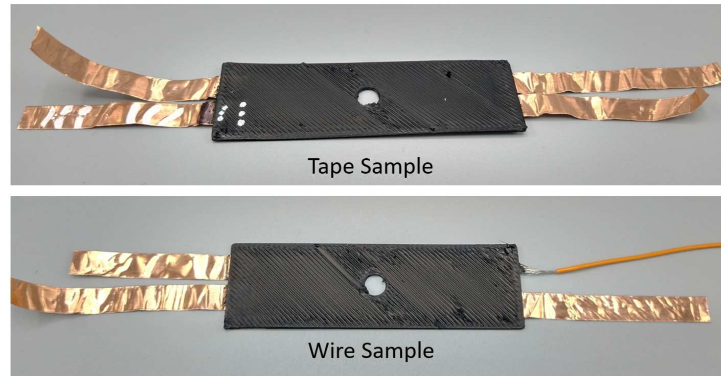

Figure 4.14: Sample used in the measurements.

4.5 Conclusion

This chapter provides a detailed account of the materials and fabrication processes employed in the creation of mechanically interlocked metal-polymer samples for subsequent mechanical and electrical performance studies. Conductive polymer used in this study was PI-ETPU 85-700+, which remains a flexible and conductive filament with unique properties. The copper tape, serving as the electrical contact was prepared using a custom punching jig for perforations. An assistance tool was developed as a necessity to address challenges in securing the copper tapes to the polymer surface in the midst of the print job, ensuring a reliable and consistent connection.

The fabrication involved aligning and embedding the copper tapes onto the polymer matrices followed by soldering to enhance the adhesion. The resulting samples exhibited mechanical interlocking and are poised for further investigation into their mechanical and electrical performances, which will be discussed in detail in the next chapter involving the experimental setup.

5 Experimental Setup And Measurements

5.1 Introduction

This chapter incorporates the details of a setup required for gathering the desired data in terms of equipment, their configuration and common procedural overview of an experiment along with the measurements performed.

Investigating the robustness of these connections when subjected to mechanical loading provide insights into long term stability and resilience in applications involving mechanical stress or deformation. Measuring contact resistance in conjunction with this provides a quantitative assessment of the functionality and reliability of electrical connections under mechanical loads. Alternatively, this also allows for a holistic analysis of the performance of the interlocking connections into how mechanical behavior impacts electrical conductivity and vice versa.

5.2 Setup Concept

The lumped models of the 4 tape sample onboard the 3-wire and 4-wire resistance measurement circuits (See Chapter 3) are considered as a foundation to the setup. The 4-wire resistance circuit involves separation of the connecting leads into specific current and voltage leads (See Figure 3.12 and 3.13, when compared to the 3-wire measurement. For the 4-wire resistance measurement, the current flows through the bottom contacts, while voltage is measured over the top contacts. In the case of 3-wire resistance measurements, the input current is switched to the top contact so that it directly flows through the top right contact under study. This is represented in a combined lumped model in Figure 5.1.

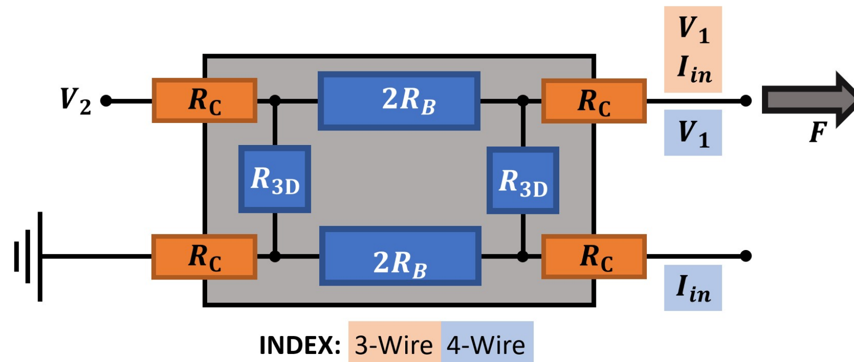

Figure 5.1: Combined lumped resistance model of the sample for both 3-wire and 4-wire resistance measurements to determine the contact resistance measurement of the top right contact. Also, simultaneously, a pulling force F is applied to the top right contact to study the behavior of the contact resistance under load.

The path of the current can be switched so that both measurements can be obtained in a very short interval of time. Incorporating an actuator to deliver a force into this circuit would constitute the skeletal measurement system as seen in Figure 5.2.

5.3 Components

With the fabricated sample and a skeletal measurement setup design, the next step is to develop a configuration to serve as an experimental setup. The main components required are enumerated:

1. Fabricated sample

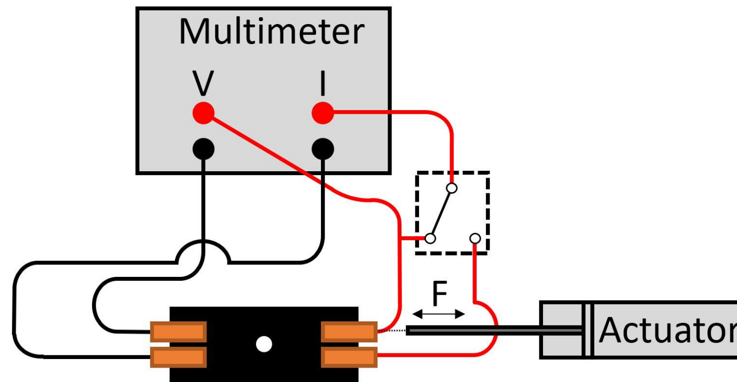

Figure 5.2: Schematic of the skeletal measurement setup with the 4 tape sample set in place to measure 3-wire and 4-wire resistance by means of a switch, in order to obtain the contact resistance of the top right tape as it is being pulled by an actuator.

2. Multimeter for 4-wire measurements - Keithley 2000
3. Linear Actuator and clamp
4. Base platform
5. Aluminum working plate
6. SMAC Controller
7. Power supply unit
8. Arduino with a 5-pin relay module for switching
9. PC - MATLAB

5.3.1 Linear Actuation and related custom parts

The SMAC LCA25-050-15E is a linear actuator with a 50 mm stroke, which can be either position or force controlled. It's working range is upto 11 N. Figure 5.3 shows the SMAC which is a large block with a metallic rod as the actuator. The SMAC can be fixed onto the working plate using mounting blocks (Figure 5.7).

Figure 5.3: SMAC LCA25-050-15E.

A PLA [70] based clamp (See Figure 5.4) is fabricated to secure the copper tape onto the SMAC actuator rod in order to be pulled. It has an M5 bolt hole in order to be affixed to the rod. It also has 2 M5 bolts all the way through the pincer region in order to tighten the gripping on the copper tape (See Figure 5.4b). The peculiar design of the clamp is better motivated using

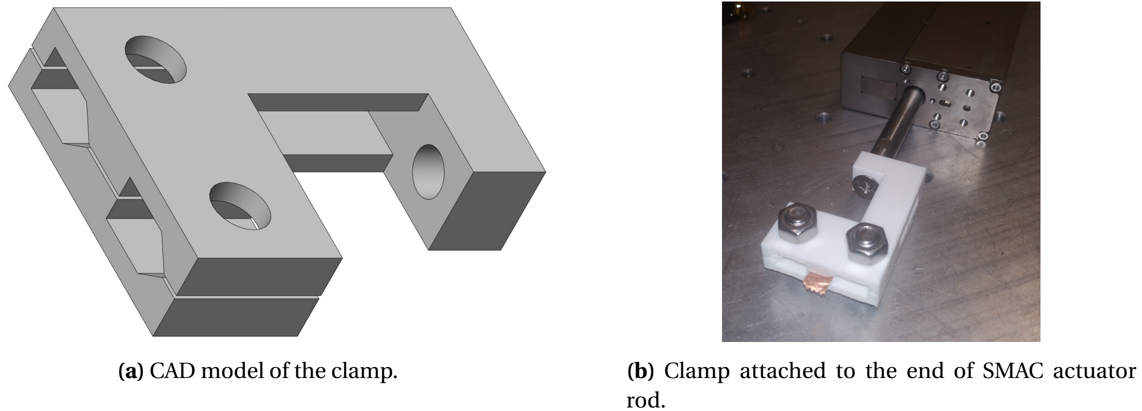

(a) CAD model of the clamp.

(b) Clamp attached to the end of SMAC actuator rod.

Figure 5.4: Clamp made of non conductive PLA.

Figure 5.5 as reference. The distance of 20 mm is provided to account for manual screwing of the actuator bolt through the bolt hole and allowing excess copper tape to continue completing the circuit. The open rectangular groove seen at the top is to be used as a pathway for wiring to be passing through without interrupting the electrical circuit. The red arrow in Figure 5.5 represents the complete coincidence of the lines of force between actuator rod and clamped section, thus removing any potential errors from offset.

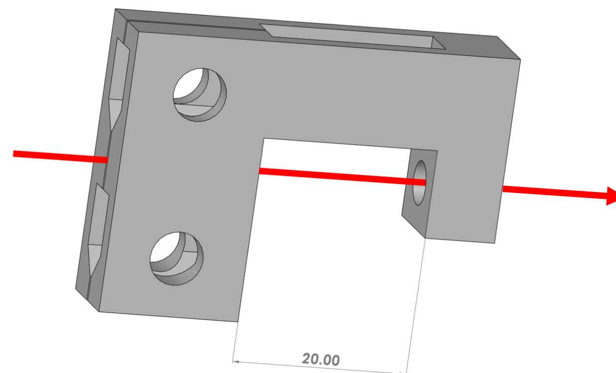

Figure 5.5: Isometric view of the Clamp. Red arrow depicts the direction of force from the actuator. Dimension is labelled in millimetre(mm).

A base platform (See Figure 5.6) is 3D-printed to secure the sample in a stationary position for measurements. It consists of multiple bolt holes to secure itself onto the working plate and holes in the centre where samples are affixed as seen in Figure 5.9a. This was designed keeping the SMAC actuator rod's height in consideration, in order to provide for a linear pulling action. This platform is also fabricated from a non conductive PLA [70]. The working plate is conductive, hence this platform serves as a non conductive conduit upon which samples can be tested without additional contacts from the external environment. Figure 5.9b shows a close up photo of the orientation of the SMAC actuator rod, clamp, sample and base platform before the initiation of any pulling force.

5.3.2 Complete illustrated diagram and Layout photo

The setup is established on top of a 50 cm x 50 cm x 3 cm aluminum mounting plate which also consists of 5 mm threaded bores placed in an ortholinear pattern along its surface. This allows for easy assembly of individual modular structures for unique experiments. Figure 5.7

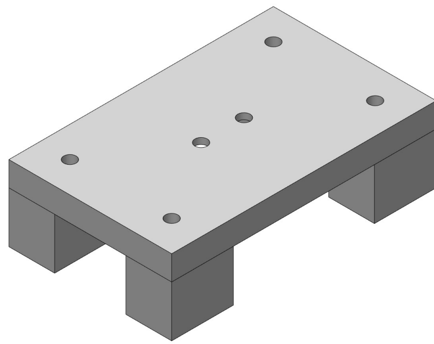

(a) CAD model of base platform.

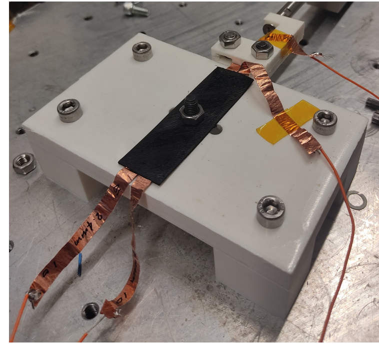

(b) 4 tape sample mounted on the fabricated base platform. The clamp attached to the actuator rod can also be seen.

Figure 5.6: Base platform made of non conductive PLA.

represents a schematic which can be used to better understand the assembly of components whereas Figure 5.8 shows the photo of the same.

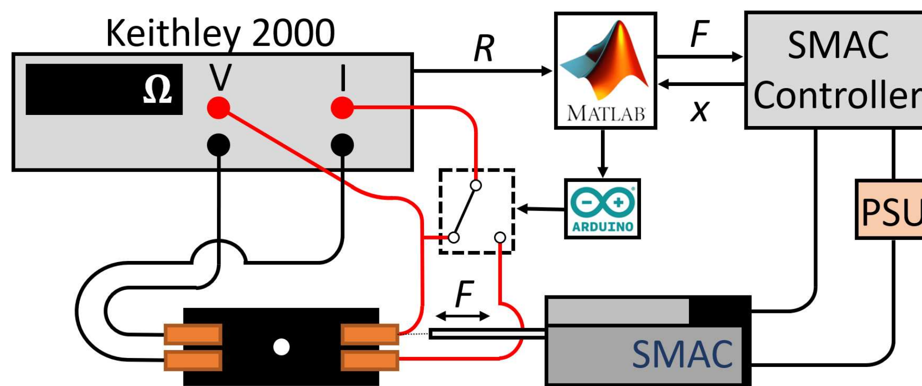

Figure 5.7: Diagram of the measurement setup.

The setup (See Figure 5.8) consists of a multimeter (Keithley 2000) for the 4-wire resistance measurement controlled through MATLAB, a linear actuator (SMAC) running a force control loop. An Arduino platform is integrated with a relay to switch one of the current terminals between two contacts in order to select either the 3-wire or the 4-wire resistance measurement circuit. Mounting blocks are used to fix the SMAC actuator onboard the aluminum work plate in a manner such that it applies a force along the copper tape axially. The 4 tape sample is bolted securely onto the base platform through a central hole in its bulk, which prevents any unnecessary translation or rotation. The copper tape (Seen in Figure 5.9a and Figure 5.9b) is clasped by the clamp, which is bolted to the SMAC actuator rod. The electrical contact from the tapes to the the measurement system is established using multimeter probes and copper wires which are soldered to the ends of the copper tapes. Various views of the experimental setup are seen in Figure 5.9. This setup remains the same for all measurements where only the sample is switched.

5.4 Measurements

This section starts of by introducing the common elements of all the measurements. These include features of the measurement circuit and physical features of the sample which remain the same throughout. Following which the measurements are discussed.

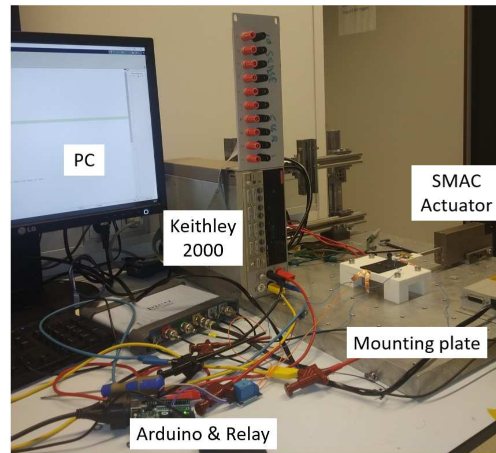

Figure 5.8: Photo of the measurement setup.

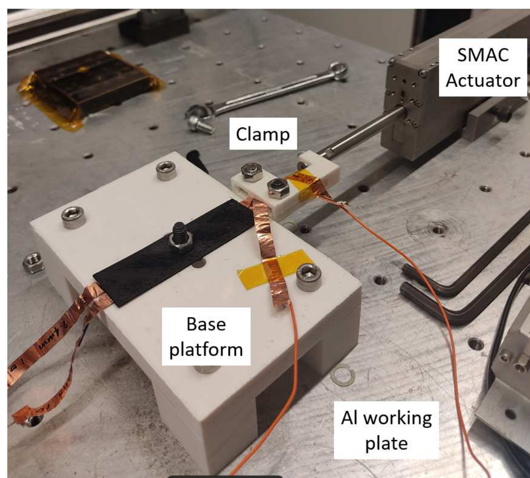

(a) Close up of the working plate depicting the sample ready to be pulled.

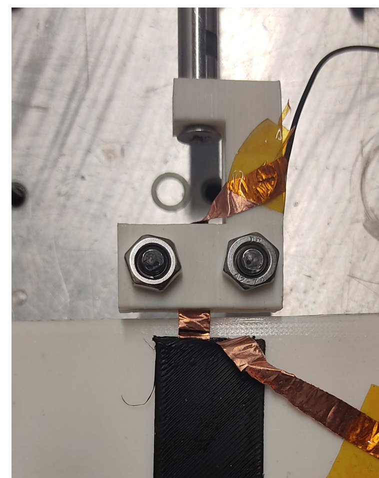

(b) Clamp clasping the copper tape prior to pulling it.

Figure 5.9: Close up of the sample depicting the copper tape clamping orientation.

All parts of the measurement setup are interfaced through the MATLAB environment, including (provided) actuator and data acquisition scripts. A small time interval is provided to initialize the Keithley 2000, the SMAC actuator and the Arduino board. The number of power line cycles (NPLC) onboard the Keithley 2000 is set to 0.1. This indicates that an input signal is integrated over 2 ms to obtain a single measurement. The relay is then powered on to complete the 4-wire measurement circuit and switched off to complete the 3-wire measurement circuit. The resistances at these instances are recorded along with the respective force and position values updated within the SMAC. This loop recurs until the force is applied over the desired time. The positional change and force applied during pulling are recorded by the SMAC actuator as negative.

Figure 5.10 depicts the physical parameters of the sample which remain the same through all the measurements performed. The zoomed in schematic of the tape depth indicates the position of the copper tape embedded in the middle layer of the ETPU bulk and is considered as the interior view. These could also be considered similarly for the wire sample, where wire depth indicates the length of the wire embedded within the ETPU bulk at its middle layer.

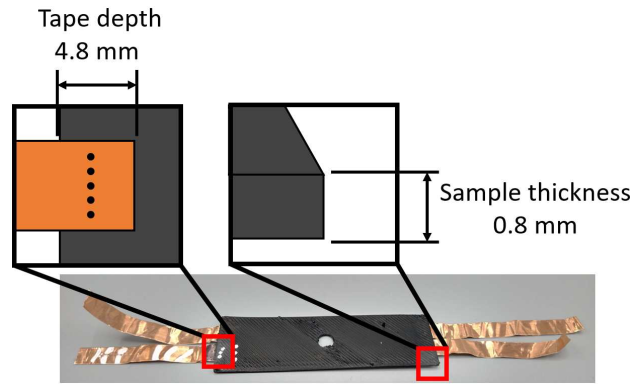

Figure 5.10: Physical parameters of the sample remaining constant in the measurements.

The ETPU bulk of all the samples was fabricated with the same print parameters. In Table 4.1 all the print parameters involved are listed. Refer to Chapter 4 for more details about the choices involved.

5.4.1 Uniaxial loading with resistance measurement

The first measurement involves the application of a linearly increasing uniaxial pulling force on both types of samples. The number of perforations on the copper tape were also varied amongst samples. The goals of these experiments were to observe the behavior at the interface of the ETPU interlocked copper tapes when a pulling force is applied. Along with obtaining insight in the resistance measurements during pulling, this provides a preliminary idea about the working range of the copper tapes with respect to the number of holes within application of the actuator's force range. Breaking points of these copper tapes based on the number of perforations could be a good indicator of the efficacy of interlocks when compared to a sample without any perforations.

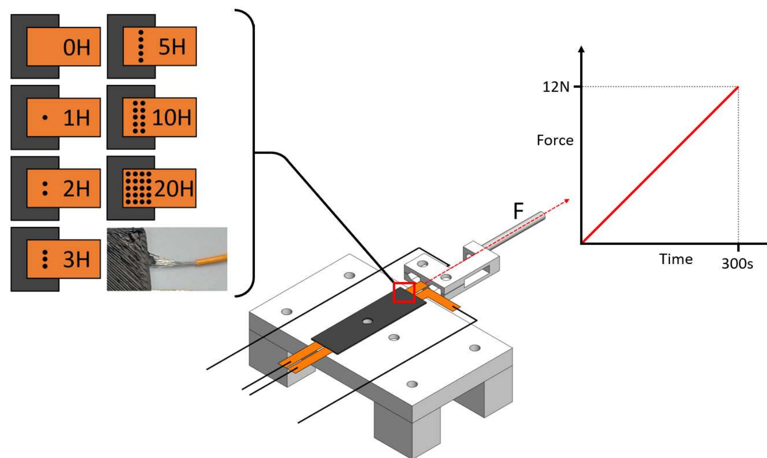

Figure 5.11: Sample utilized with various hole configurations.

The number and pattern of perforations on tape samples are shown in Figure 5.11. Tape samples with the following number of perforations are considered: 0, 1, 2, 3, 5, 10 and 20. Along with this, 2 wire samples are also considered. To ensure consistent and reproducible testing, the samples were securely bolted onto the platform. A uniaxial pulling force increasing linearly from 0 N to 12 N over 300 seconds is applied on the samples (See Figure 5.11), while measuring the 3-wire and 4-wire resistances. This is in line with the objectives of this research, simulating

a gradual, incremental force reflecting the mechanical stresses these contacts might experience in practical applications. Samples undergoing structural failure during these loads can be visually inspected to better understand the failure mechanism of the mechanical interlocking.

5.4.2 Cyclic Loading with resistance measurement

Moving on, samples are subjected to a cyclic triangular force profile over an extended period, allowing for study under repetitive loading conditions. This approach is aimed to gain a better understanding of contact resistance in flexible conductors during cyclic loading, which is primal in various applications.

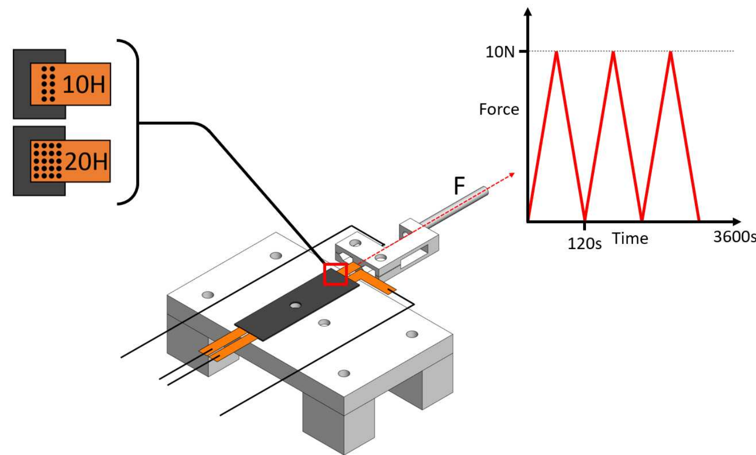

Figure 5.12: Sample utilized with various hole configurations.

Figure 5.12 also depicts the number and pattern of perforations on the tape samples. Only tape samples with 10 and 20 perforations are considered. The cyclic loading profile consists of a triangular waveform ranging from 0 N to 10 N, with a loading rate of $\pm\frac{1}{6}\,\mathrm{N\,s^{-1}}$ (See Figure 5.12). The time period of this wave is 120 s. This cyclic loading is maintained for a duration of 3600 s, allowing for the study of the sample's response to a significant number of loading cycles.

5.5 Conclusion

Based on the development of the lumped model from Chapter 3 and fabrication of samples from Chatper 4 and a few custom fabricated parts, an experimental setup is designed. This is required to secure fabricated samples and perform simultaneous force and resistance tests. Details of significant constituents and the functionality of the measurement system are established. Along with a preface of the necessary parameters, types of samples involved and common procedures, an overview of the performed experiments utilizing a uniaxial and triangular force profile is presented. The results of the measurements are presented in the next chapter.

6 Results

6.1 Introduction

This chapter houses the results of the two experiments in sequence as mentioned in Chapter 5. The goals are to obtain insight in the nature of the interlocking region between the polymer and copper tape and to measure the breaking point of samples, identifying influential parameters, estimating contact resistance from individual resistances and to identify its behavior through the types of loading on the samples. This will address both the mechanical and electrical characteristics of the sample.

6.2 Mechanical interlock interface

A fabricated sample is sliced through its cross section with a scalpel in order to have a look at the copper-polymer interface where the interlocks occur. Figure 6.1 depicts the sliced cross section of a sample and a close up of the interlocking occurring in multiple samples. This form of destructive testing is an easy way to identify the quality of the sample so far.

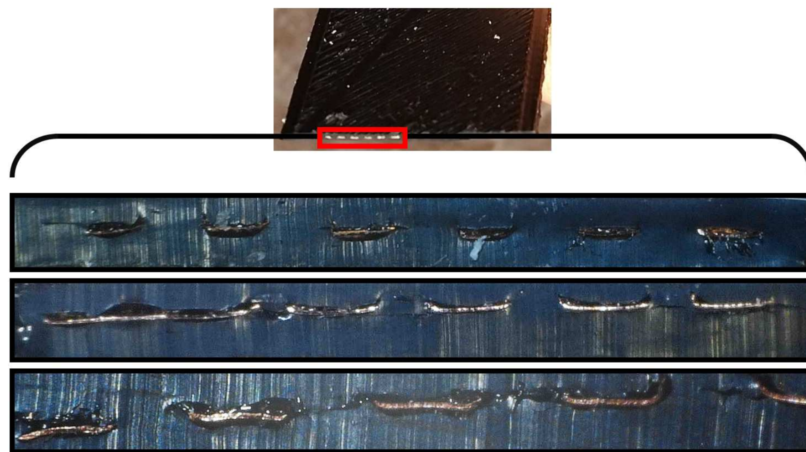

Figure 6.1: Cross section of a sliced sample along with microscopic images of the cross sections of multiple samples. [19].

The microscopy clearly shows polymer extruded through the perforations in the tape. Sufficient fusion between the top and bottom halves of the polymer layers was observed despite there is considerable time passing between pausing the extrusion, mounting copper tapes and resuming the job. Clearly, some voids are visible in the immediate proximity of the copper tape. These form ridges along the interface between copper and polymer. The copper tapes occurring bent or with a curved "U" shape is due to the punching action from the jig whose impulsive force can bring about such changes. This shows that there can be considerable grounds for improvement in the quality of interlocking which is further discussed in the Future Recommendations in Chapter 8.

6.3 Uniaxial Loading Measurements

In this section, the results of uniaxial loading upon the samples, which was discussed in subsection 5.4.1, are shown. The results are focused on the position of the tape, the simultaneously measured 3-wire and 4-wire resistances, the contact resistance between the copper tape and polymer and the breaking points of the samples.

6.3.1 Positional measurements and breaking point

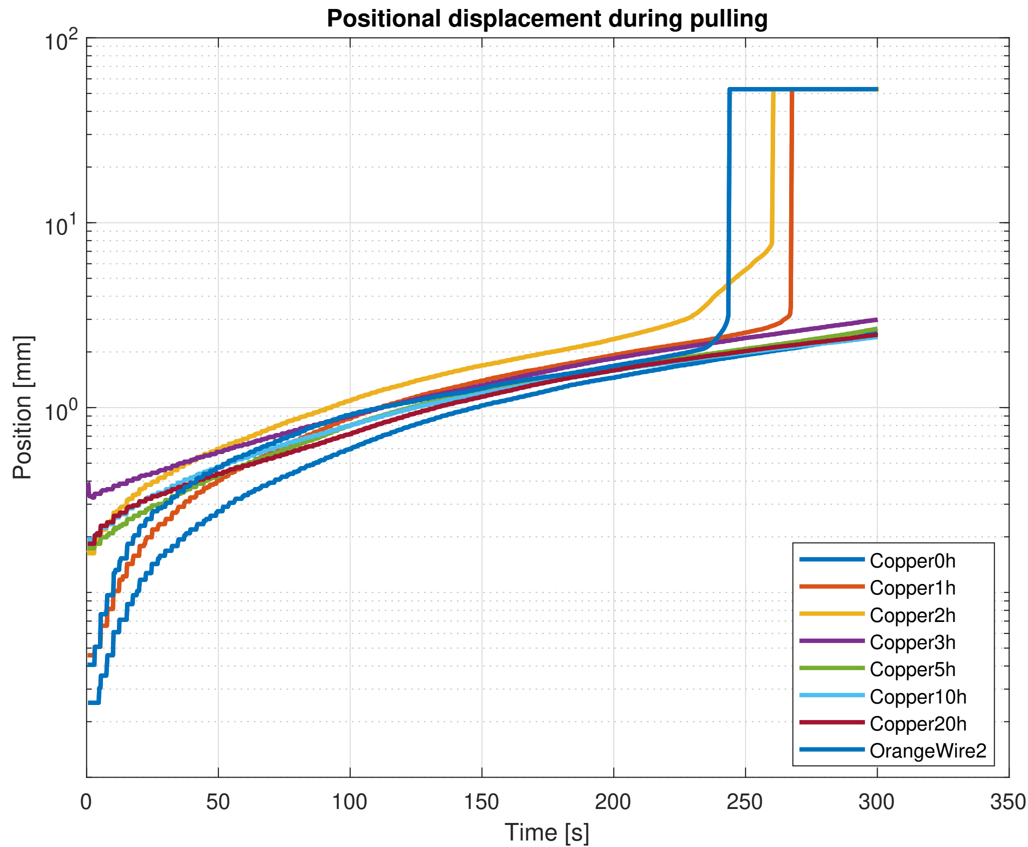

Figure 6.2: Positional change of copper tapes when pulled uniaxially with a linearly increasing force from 0 N to 10 N. The near instantaneous vertical climb indicates structural failure of samples. OrangeWire2's color index is blue ,located topmost (verified by Figure 6.4)

Positional changes were noted for every sample, however most interesting are ones which encountered structural failure with regards to either the tape or the polymer stake within the perforation. Figure 6.2 show the position versus time measurements of 4 samples. Captions for Figure 6.2 and Figure 6.3 clarify the blue colored index usage for the wire and tape sample with 0 holes.

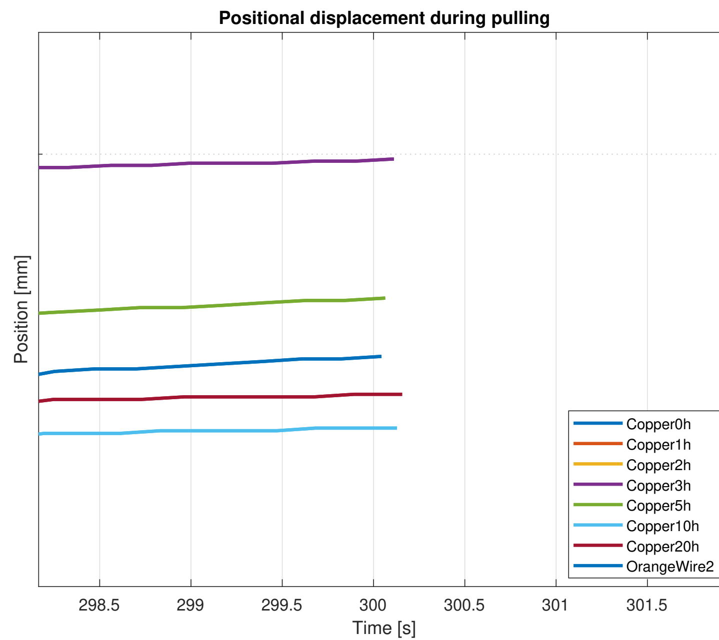

Figure 6.3: A zoomed in section of Figure 6.2 which depicts the samples where copper tape did not slip out of the matrix at the end of the test. Copper0H's color index is blue, located in the middle.

From Figure 6.3, it is observed that copper tape with 10 and 20 holes underwent the least positional change during pulling. This demonstrates their resilience to load. Following by closely are tapes with 3 and 5 holes. The sample with embedded wire failed the earliest, even before the tapes with 1 and 2 holes. While an anomaly was observed with the tape with 0 holes, further consideration in required to study the effect of having no perforation but merely relying on soldering.

The forces depicting the breaking point of the wire and 1 hole sample are shown in Figure 6.4 and Figure 6.5 respectively. This can be a very basic proof of the potential mechanical interlocking can have when compared to the conventional wire embedding that is widely used.

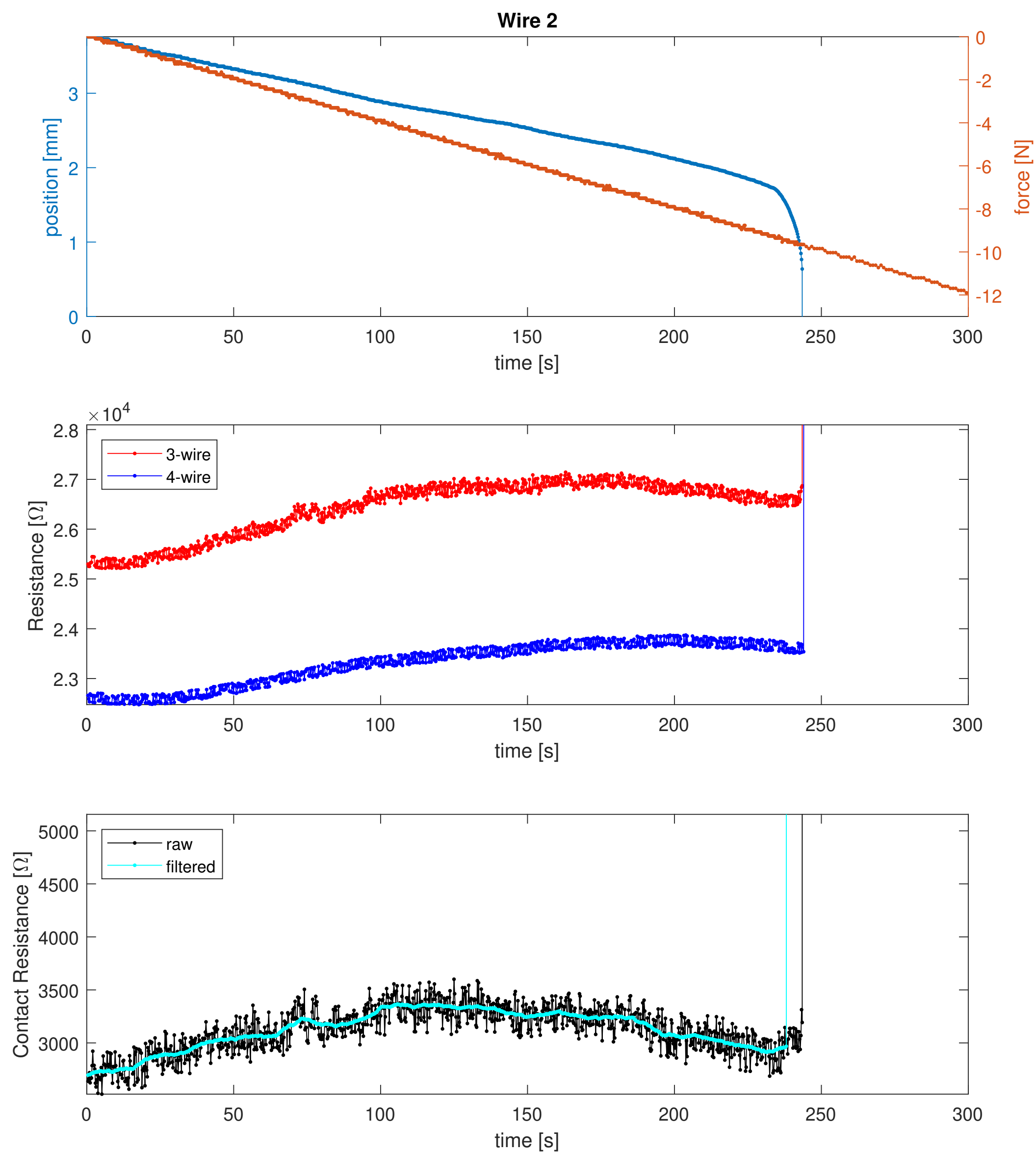

Figure 6.4: Results for wire sample: Position and Force over time (top), 3-wire and 4-wire resistance versus time (middle) and their difference versus time (bottom).

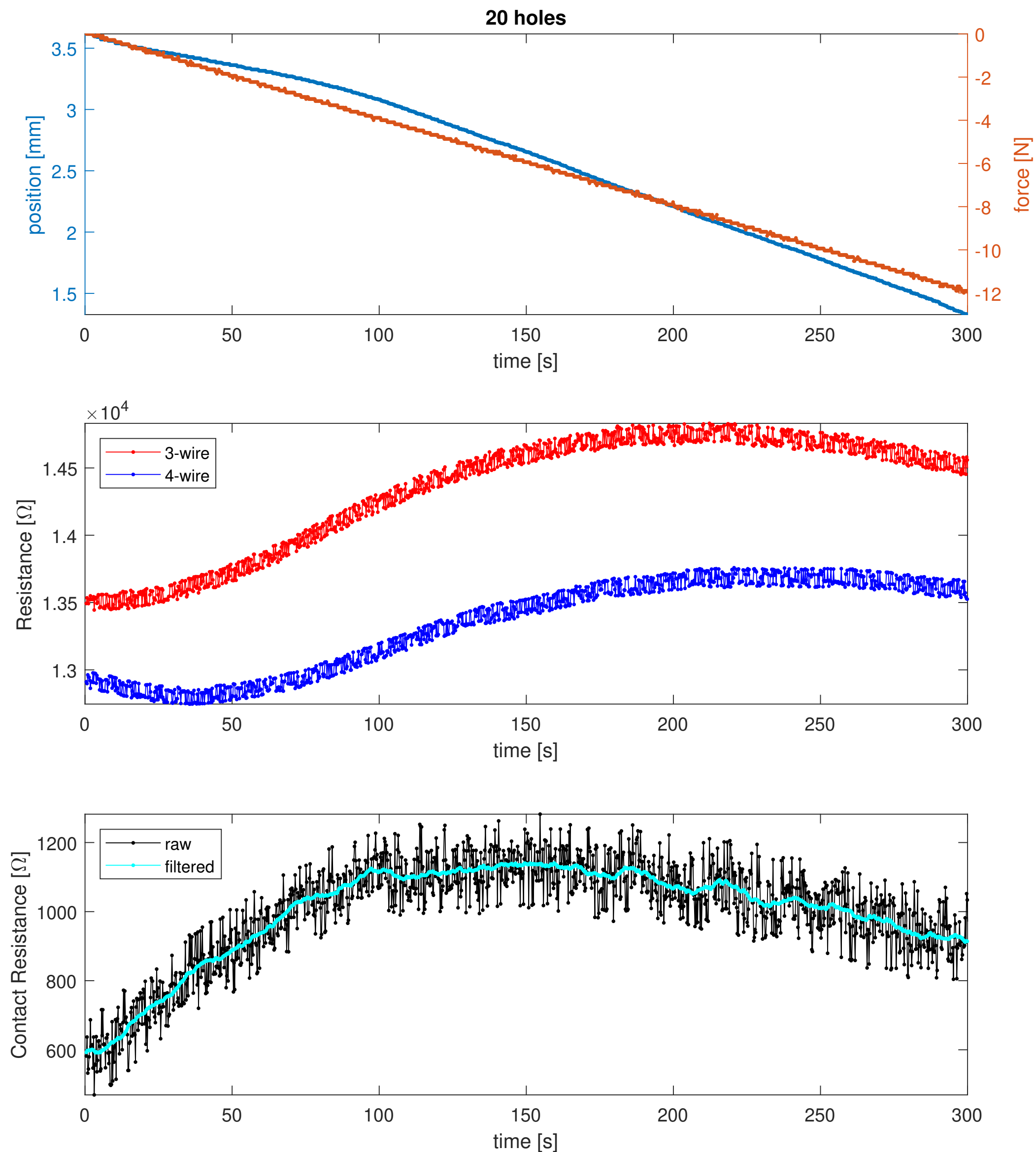

Figure 6.5: Results for 20 hole sample: Position and Force over time (top), 3-wire and 4-wire resistance versus time (middle) and their difference versus time (bottom).

Additionally, copper tape with no holes slipped out of the polymer matrix. Without any form of interlocking, this sample only relied on the immediate adhesion from the melting of polymer in its proximity from the soldering effect.

Figure 6.6 depicts the clamp pulling a copper tape with 1 hole before it broke away from the polymer matrix. A pit is formed which depicts the individual polymer stake which is being pulled directly through the tape. While the pit is observed in the top layers, the stake is clearly 4 layers below. This pit could be a result of the polymer stake in strong contact with the upper layers of the matrix as well. This observation was not present in any other samples. This could potentially mean that the distribution of the pulling forces on multiple polymer stakes hap-

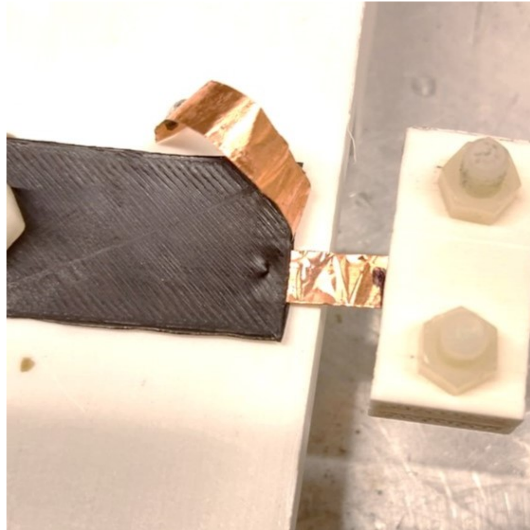

Figure 6.6: Pit formed due to the polymer stake being pulled through the singular hole of the copper tape under loading.

pens uniformly. This is evidence that mechanical interlocking through the copper tape indeed withstands the load provided physically.

Figure 6.7 shows the aftermath of breaking points on the copper tapes on samples consisting of 1 and 2 holes. Two possible ways of failure in this situation involve breaking of polymer stake or tears in the perforations.

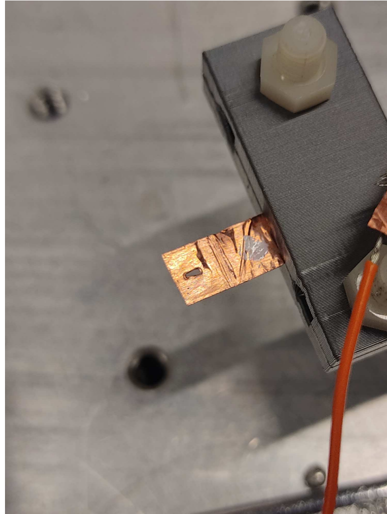

(a) The intact hole depicts the failure of the polymer stake passing through it, thus letting the copper tape slide out of the polymer matrix. Plastic deformation is observed.

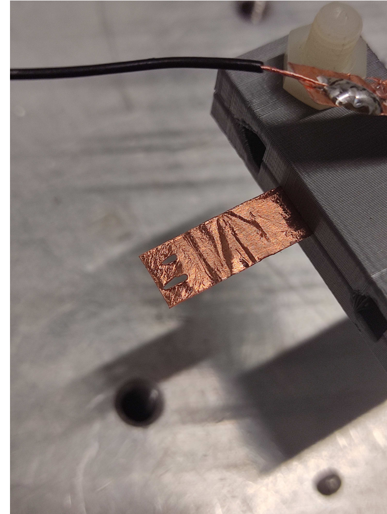

(b) The tape depicts 2 holes which are deformed from pulling. The tape is not torn off, which indicates the failure of the polymer stake.

Figure 6.7: Close up of copper tapes depicting the state of 1 hole (left) and 2 hole (right) perforations after slipping out of the polymer matrix.

Figure 6.7a shows how the individual perforation remained intact while the tape slipped away from the matrix. This indicates that the polymer stake must have broken off or would have been sliced by the surrounding copper tape along with the pulling force. This can be observed in Figure 6.8, where the stakes have been sliced with only short stubs remaining. Figure 6.7b also depicts the same aftermath involving a tape with 2 holes. Two potential scenarios for failure are

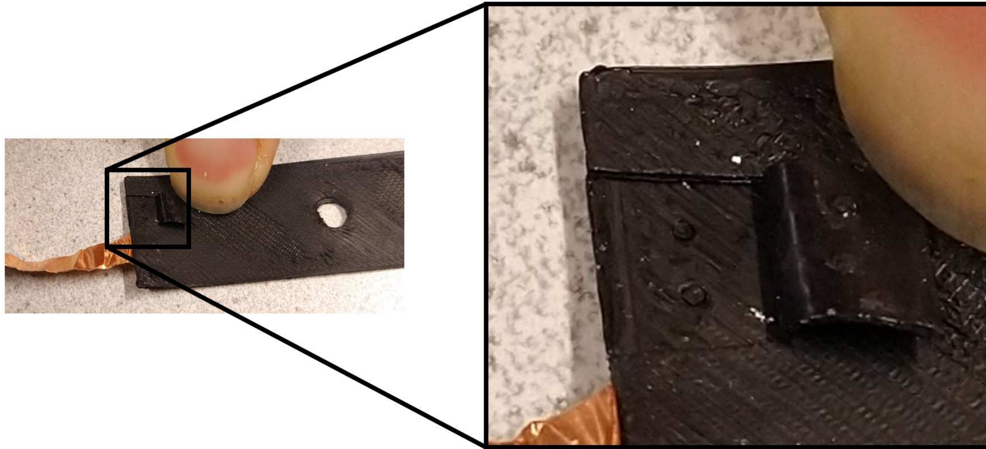

Figure 6.8: Close up of polymer matrix after pulling out the copper tape, depicting two broken polymer stakes.

better explained in Chapter 7 under subsection 7.5. Interestingly, in both scenarios the holes are slightly elongated through pulling. This is evidence of the polymer stakes resisting the pull, thus causing these deformations in the holes.

6.3.2 Resistance measurement

Figure 6.9 shows that the tape with 1 hole has a breaking point of around 10.5 N at around 265 seconds while Figure 6.4 shows the wire sample has a breaking point of around 9.6 N occurring at 242 seconds.

The behavior of resistances in both the specimens starts off with a small dip at the start of pulling action, followed by a rise in the resistance. Near the point of breaking, the resistance unexpectedly decreases. Potential underlying phenomena behind this are explained in Chapter 7. However, the 4-wire resistance data already shows that the wire has a greater starting resistance than either of the tapes.

It is also interesting to note the decrease in the 4-wire resistance value of the 20 hole sample (See Figure 6.5) when compared to the 1 hole sample at the start of the measurement.

Figure 6.10 shows the change in the difference between the 3-wire and 4-wire resistance $R_C + R_{3D}/2$ before pulling and the normalized contact resistance approximation $(R_C + R_{3D}/2)/R_b$ during pulling . While these results do not show a direct relationship between the number of holes and contact resistance R_C, but it does go on to show that R_C is within a couple percent of the sample resistance. With increasing force, $R_C + R_{3D}/2$ initially climbs and then descends, which is observed on all the samples except the tapes with 1 and 2 holes which broke away from the sample. The change in resistances is observed to be higher for the wires when compared to the tapes. This could also be due to the resultant increase in the spacing between the wire and proximal tape, when compared between samples consisting purely of tapes [19].

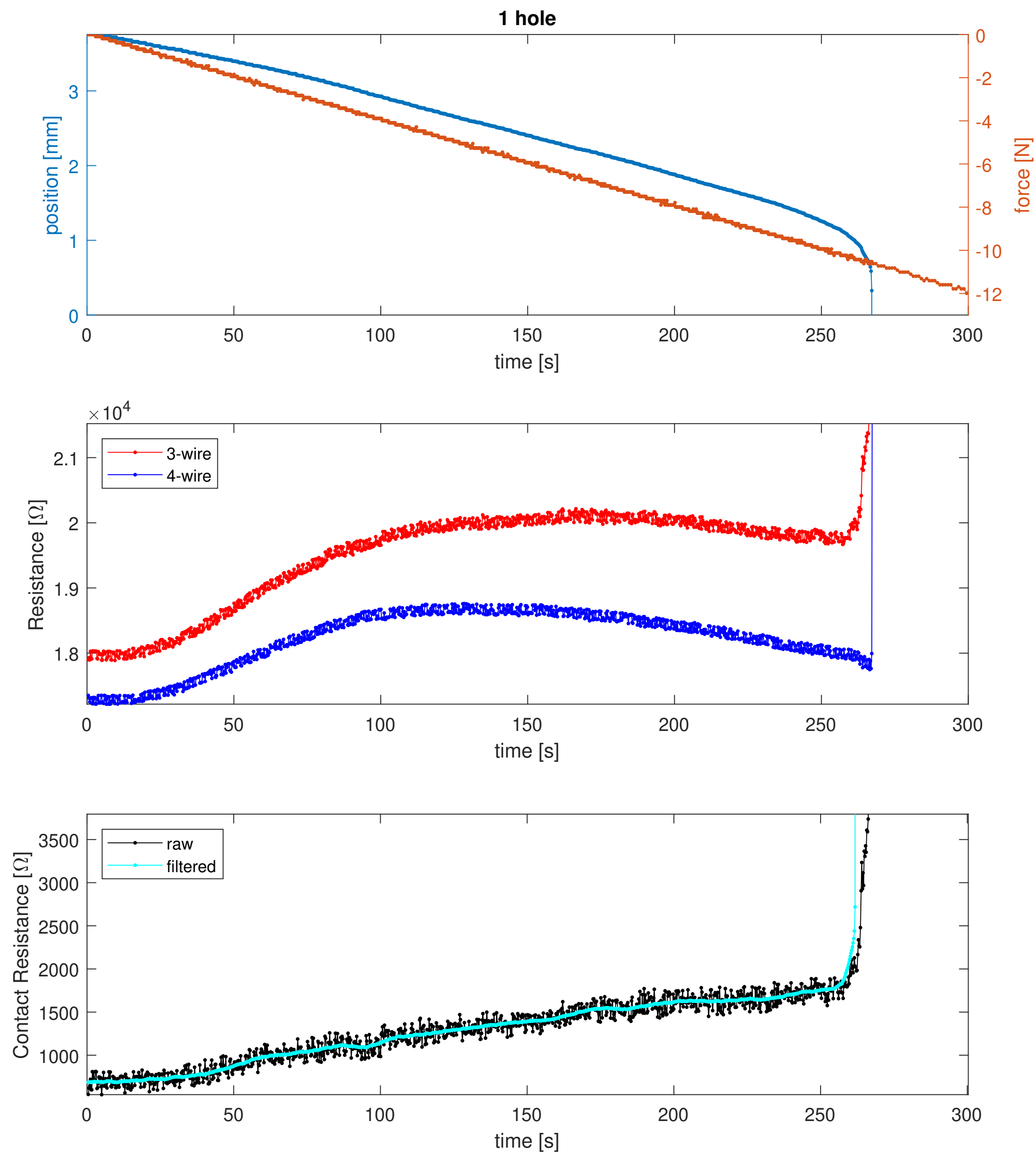

Figure 6.9: Results for 1 hole sample: Position and Force over time (top), 3-wire and 4-wire resistance versus time (middle) and their difference versus time (bottom).

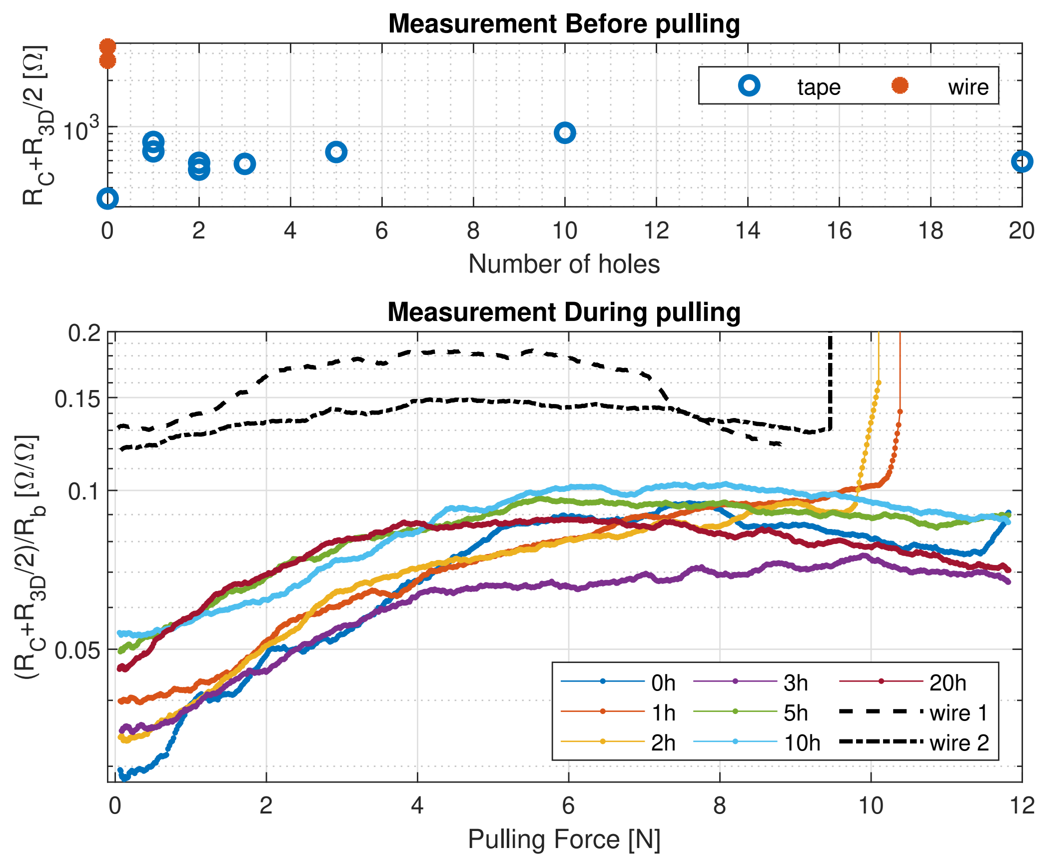

Figure 6.10: The difference in 3-wire and 4-wire resistance measurement before pulling (top) and contact resistance approximation while pulling (bottom).

6.4 Cyclic loading measurements

The results of cyclic loading, which was discussed in subsection 5.4.2, are shown. The results are focused on the positional change and force experienced by the tape, the 3-wire and 4-wire simultaneous resistances, contact resistance between the copper tape and polymer over time. The period of the cyclic triangular signal is 120 seconds, with a gradually increasing pulling force from 0 N to 10 N and decreasing back to 0 N. The negative symbol once again represents the action of pulling.

6.4.1 Positional and resistance measurements

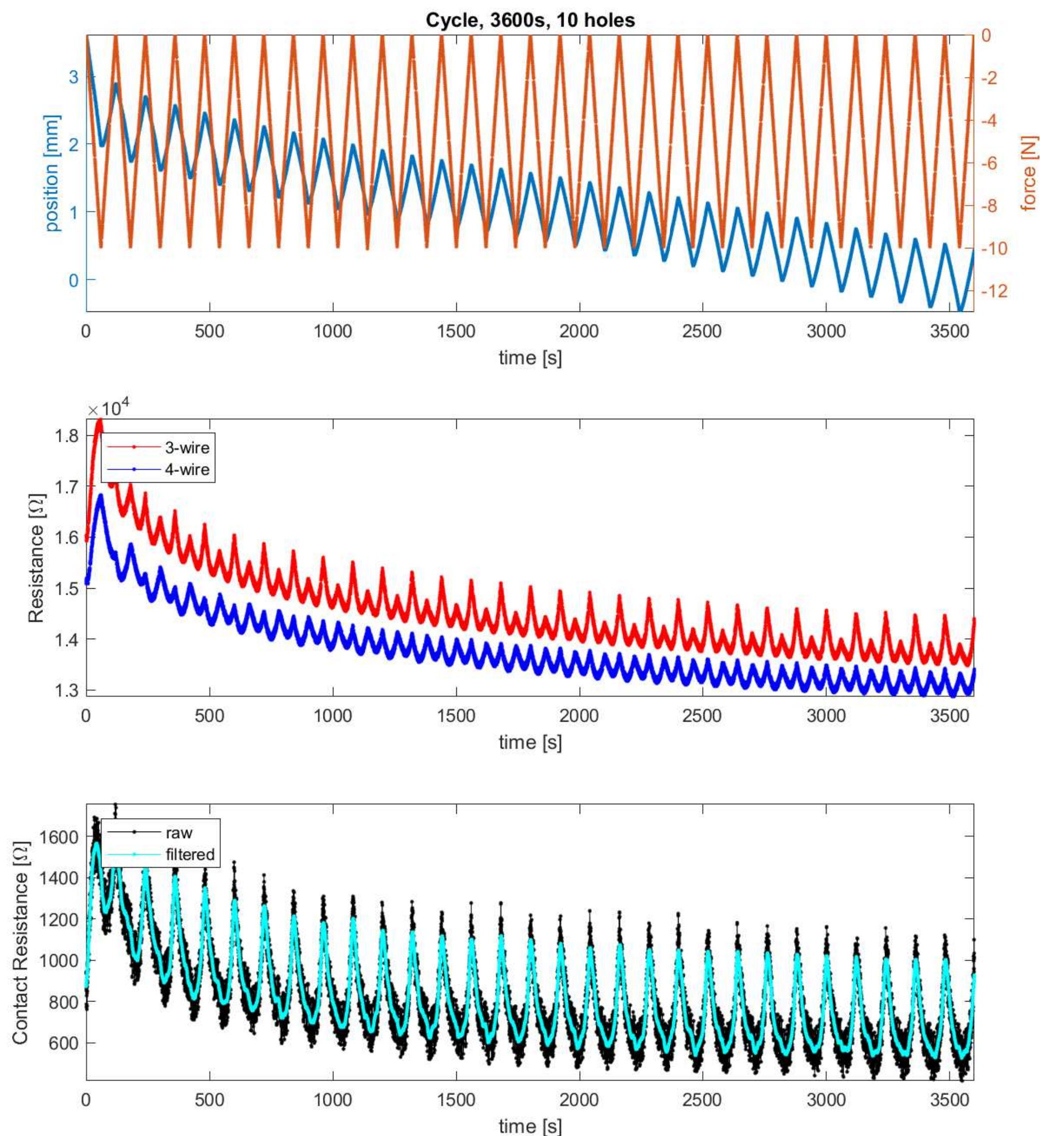

Figure 6.11: Results for 10 hole sample: Position and Force over time (top), 3-wire and 4-wire resistance versus time (middle) and their difference versus time (bottom).

Figure 6.11 shows a multitude of cycles for the sample with 10 holes and Figure 6.12 depicts the same for the sample with 20 holes. In Figure 6.12, a sudden reduction in the noise is observed at around 2500 s, which is unaccounted for now.

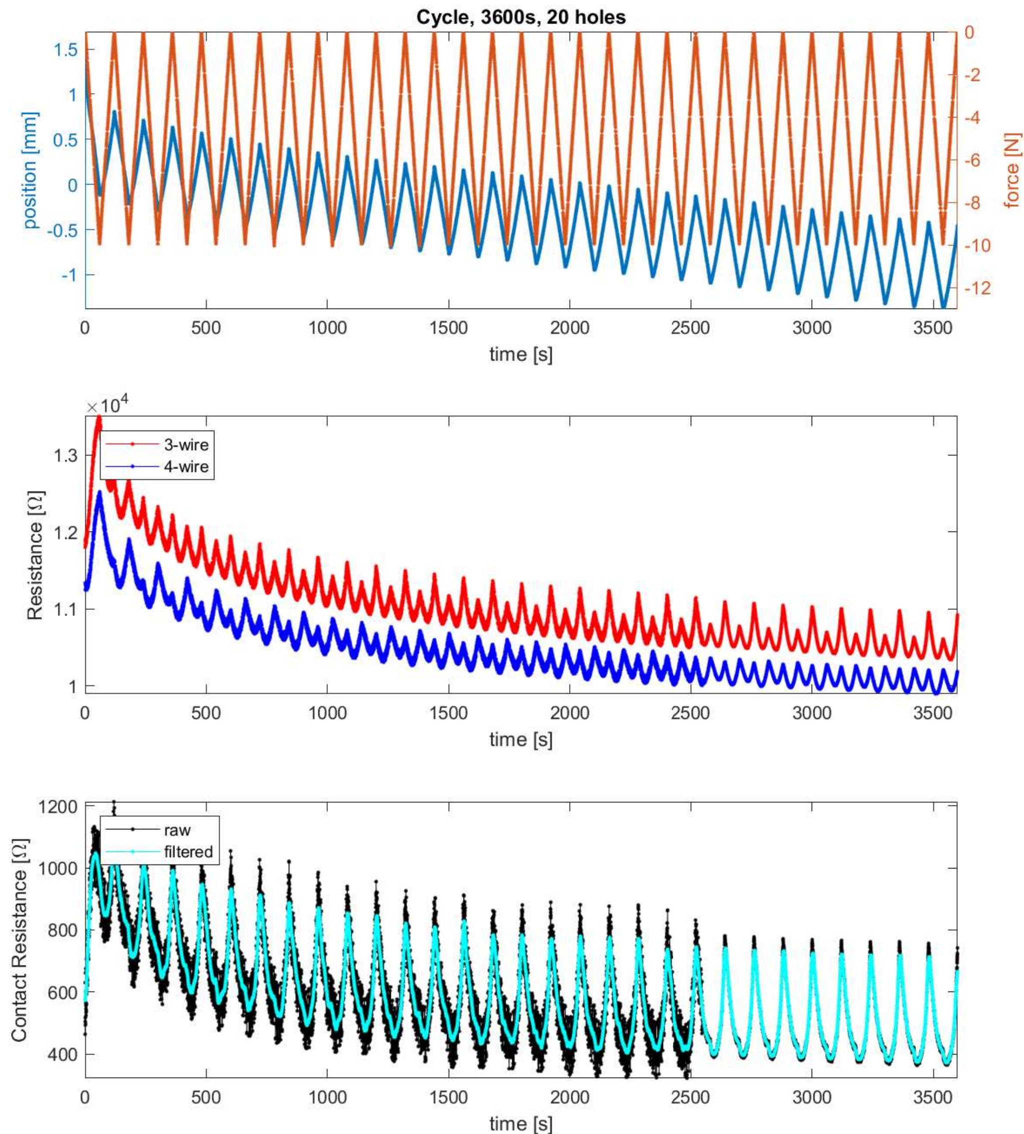

Figure 6.12: Results for 20 hole sample: Position and Force over time (top), 3-wire and 4-wire resistance versus time (middle) and their difference versus time (bottom).

Neither of the samples broke off during 30 cycles of measurement spanning an hour. From the results obtained in subsection 6.3.1, it can be once again predicted that a tape with 20 holes is expected to resist load better than a tape with 10 holes. Clearly, that is also observed in the results. Over a time period of 3600 seconds, the tape with 10 holes has moved 3.2 mm. The tape with 20 holes has moved 1.4 mm. This is calculated by noting the change in the initial and final peak of the positional response. However, this occurance can be due to a combination of copper tape deformation along with slippage within the grasp of the clamp. This is also a potential indicator of how many cycles a sample can withstand before reaching its breaking point. In this

specific case, twice the number of holes clearly showed half the position change. Greater number of holes accommodate a larger resistance to the cyclic load, thus gives a nascent promise to explore this with greater number of holes in the future.

The starting 4-wire resistance of the 20 hole sample is also lesser than the 4-wire resistance of the 10 hole sample. It can be observed that during the pulling force from 0 N to 10 N in each half cycle of the wave, the resistance appears to behave similar to what is observed in Figure 6.10. There seems to be a minute stable zone followed by an increase in the resistance as the pulling force increases. The gradual offset is observed wherein the resistance decreases with time.

Figure 6.13 depicts the normalized contact resistance approximation for the tape with 10 holes with respect to the force applied along with time.

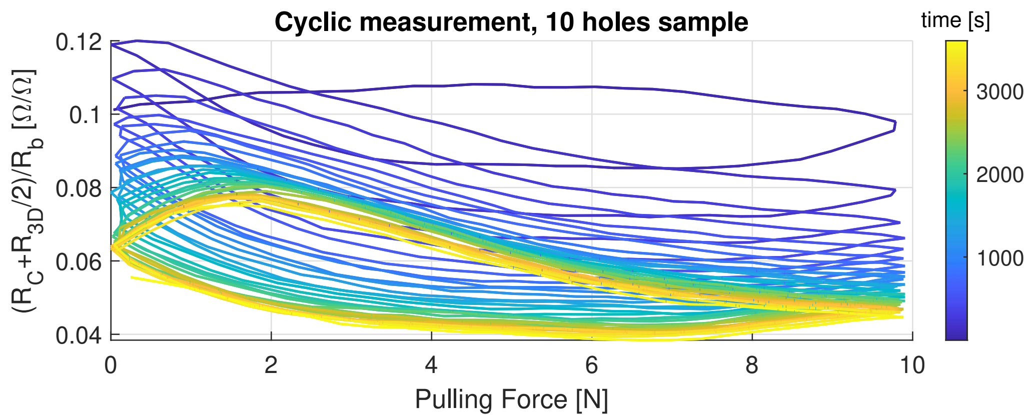

Figure 6.13: Difference between 3-wire and 4-wire resistance with respect to the cyclic load on a 10 hole copper tape. The loop runs clockwise with time indexed by the colored bar on the right.

A stable clockwise, hysteresis loop is observed. Moreover, contact resistance decreases after pulling, which can be theorized to be caused to an improved contact at the interface between ETPU and the copper tape. A drift is observed before the cyclic measurement stablizes which could be explained by creep.

6.5 Conclusion

The cyclic tests depicts the change in robustness with varying number of holes under repeated loading. Mechanical failure occurred for tapes with 1 and 2 holes, with the polymer stake having been broken. From the results, it can be seen taht these two samples performed better than a wire sample as well. The contact resistance is first observed to generally increase with the beginning of the load, following a gradual decrease. Contact resistance is also noted to be accounting for only a few percent of the sample resistance, thus establishing a foundation for further research into how mechanical interlocking can be suitable for applications onboard flexible and conductive systems.

Also, there is no clear indication of contact resistance reliance on the number of holes. That being said, while the parasitic component of the resistance $R_{3D}/2$ is prevalent, contact resistance is relatively low and stable under large periodic loads.

The behavior of samples during loads are discussed in Chapter 7, which could be a reasonable explanation for the observations. These measurements also bring into question, to ponder for ways to fine tune the experimental setup, alternative methods for better estimation of contact resistance and better forms of analyzing the parasitic and bulk resistances that are part of the

samples. A variety of these are also mentioned in the future recommendation part of the Chapter 8.

7 Discussion

The preceding chapters have ventured towards achieving a reliable connection between metal and polymer, beginning with an analysis of the design, fabrication, experiments and results. This chapter serves to explain key concepts and mention potential correlations based on the obtained results.

7.1 Copper tape versus copper wire

The results obtained from this study indicate that there are significant differences in the mechanical and electrical behavior of copper tape and copper wire samples. The tape samples clearly demonstrated a higher degree of mechanical bonding presumably due to the effective interlocking between copper and ETPU, when compared to the wire samples. This is evident from the higher pull-out force required to remove the tape samples from the polymer matrix when compared to the wire samples.

In terms of electrical behavior, the tape samples showed a lower resistance compared to the wire samples. This could be attributed to the larger surface area of the embedded tape, which allowed for a greater contact area between the conductive polymer and the copper tape. This resulted in a lower resistance path for the current to flow through, which clearly impacts the performance of the system.

However, it is important to note that the tape samples also showed a higher degree of variability in their mechanical and electrical behavior. One probable cause can be attributed to the perforation mechanism used to create the holes in the tape, which resulted in some degree of bending and deformation of the tape as seen in Figure 6.1. The amount of deformation varies with every perforation and quality of the interlock with the proximal ETPU layers.

While more number of samples need to be tested statistically in order to obtain more concrete results, so far the results do favor copper tape in being a more effective method for connecting metallic conductors to conductive polymers. Along with the recommendation to optimize the perforation mechanism, it can be worth to investigate the long-term stability and durability of the interlocking mechanism for both tape and wire samples to determine their suitability for specific practical applications

7.2 Role of the perforations

The holes on the copper tape embedded within the ETPU matrix play a crucial role in the mechanical interlocking mechanism. The stakes that occur when the polymer flows through the holes create a strong mechanical bond between the metal and polymer, which enhances the overall strength and durability of the connection.

The size, shape and distribution of the perforations can significantly affect the mechanical properties of the connection. Greater number of perforations mean greater number of polymer stakes which resist the pull of the copper tape, thus improving the load bearing capacity of the connection.

It is also important to consider the potential side effect in amassing a large number of holes on the copper tape could weaken the structure in general and may amount to tearing or structural failure of the tape during pulling. Optimizing the number of holes while also taking other details into consideration can pave way for desirable performance.

7.3 Difference in thermal expansion between ETPU and copper

It is clear that ETPU remains a flexible polymer and its thermal expansion coefficient is higher than that of copper, which means that ETPU expands or shrinks more than copper when subjected to a temperature change. This is the underlying theory that can explain why the interlocks between ETPU and copper work well.

During the printing process, the copper tape mounted onto the polymer matrix is subjected to heat from the bed and soldering iron (Explained in Chapter 4. The first half layer of the base ETPU layer melts, thus allowing for the copper tape to be anchored. This is in addition to smearing some polymer onto the tape boundaries to further secure it. Molten polymer is then extruded onto the tape, which flows through the perforations and fuses with the base layer. Upon cooling, ETPU hardens and solidifies within the perforation, thus allowing for the formation of stakes. This mismatch in the thermal expansion coefficients between ETPU and copper could promote a shrink fit within the perforation, where post cooling, the effective contact area at the interface between these materials could increase. The stake likely undergoes contraction and pulls the ETPU against the contacting copper tape. Hence, it is critical to consider the thermal expansion of the materials involved while designing and optimizing the connection, along with maintaining supportive ambient temperatures such as the printing bed.

7.4 Contact points between copper and polymer during pulling

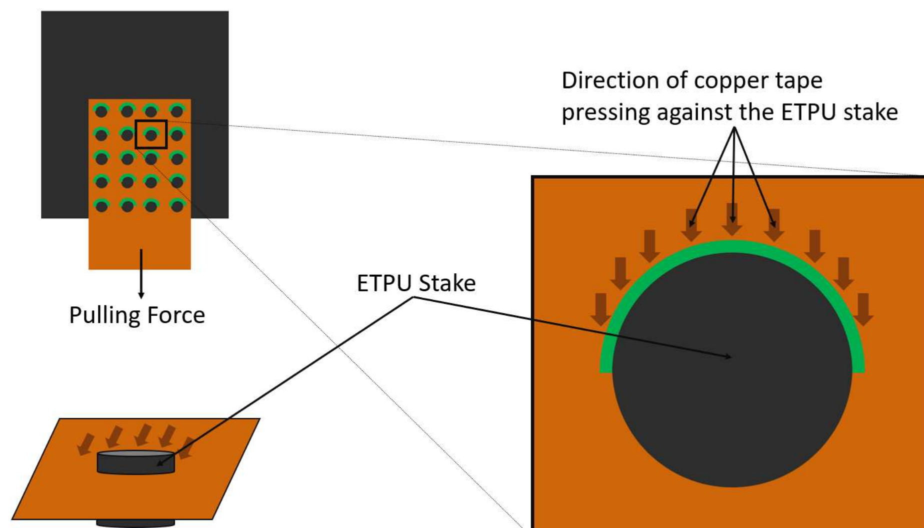

Figure 7.1: Multiple views of the macro level interface between perforated copper and ETPU stakes through it. The green arc indicates the region where contact could be enhanced due to the tape being pressed against the surface of the ETPU stake.

When perforated copper tape is pulled in one direction, several underlying behaviors can be considered at the interface between the copper tape and the surrounding ETPU regions, some of which could particularly impact the measurement of contact resistance. A pit formation was observed during pulling as seen in Figure 6.6. As seen in Figure 7.1, there could be an increase in the contact area between the copper tape and surrounding ETPU along the direction of the applied force. This could result in improved electrical conductivity at the interface thus implying reduction in contact resistivity, which is a desired parameter for use in respective applications. However, it is also important to consider that on the other side of the arc, copper tape may correspondingly move away from the ETPU stake, thus more observational research is necessary to aptly identify these changes as linear or non linear.

Pulling of the copper tape with ETPU enveloped all around can influence further responses within the interface. Deformation, stress concentrations, increased friction and change in orientation of polymer chains are some of them. Specific behavior is again dependent on the material properties, geometry of perforations, magnitude and direction of applied force and rate of pulling. As discussed previously, the number of holes and the amount of copper tape embedded within the bulk of the ETPU matrix could very well affect the contact resistance as well. Experimental testing could give a deeper understanding of these interactions and can further assist in optimizing the design for improving the desired performance factors.

7.5 Failure point scenario

To understand the points of failure, we consider an individual hole encompassing a polymer stake as shown in Figure 7.2. This occurs at every instance of perforation located on the tape in the experiments performed, prior to initializing the pulling force.

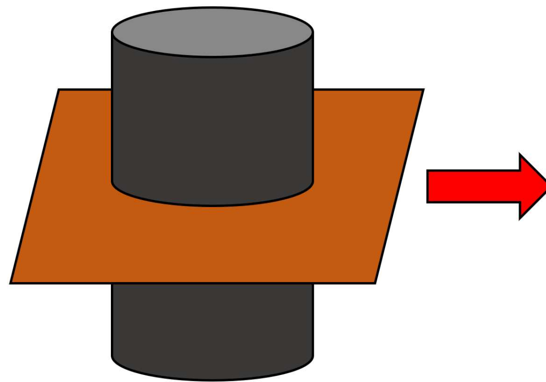

Figure 7.2: Schematic depicting the state of polymer stake through the perforation on copper tape before pulling. The red arrow indicates the direction of pulling force

Figure 7.3 depicts two instances of failures along with the polymer-tape interlock schematics. The first case as shown in Figure 7.3a is corresponding with the result obtained in Figure 6.7a. Along with some plastic deformation, the hole on the copper is still intact after it is pulled away from the polymer matrix. Probably explanation would amount to breaking of the polymer stake that was embedded within the hole. A potential reason for the breaking is that the copper tape could have sliced through the polymer stake, most probably in the case of a thinner polymer stake which could be classified as a weaker interlock occurring at the hole [15, 56].

The second case as shown in Figure 7.3b is with regards to the result obtained in Figure 6.7b where the two hole sample broke away from the polymer matrix with a structural failure occurring on the tape. The polymer stake would have to be structurally intact for the most part, in order to tear through the copper tape. From the results, there has been enough evidence that greater number of holes amount for greater breaking force required. The tearing as seen in Figure 6.7b could be due to the fact that two polymer stakes were interlocked with the tapes thus giving a greater physical resistance to being pulled when compared to the tape with 1 hole. This resistance could have been too much for hole around the stake to withstand and thus had to break away.

7.6 Estimation of R_{3D}

From designing a lumped model of the sample in subsection 3.3.3 in Chapter 3, it was known that the change in the resistances of the 3-wire and 4-wire measurement amounted to the contact resistance R_C and a parasitic resistance R_{3D} (Equation 3.9). Figure 7.4 depicts the geometrical dimensions of the sample along with the lumped model. Using this as reference, a purely

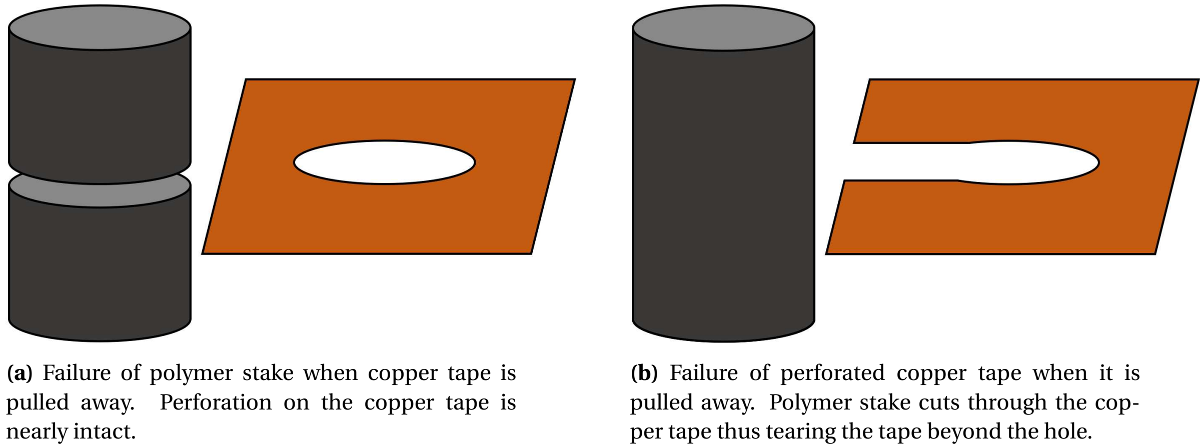

(a) Failure of polymer stake when copper tape is pulled away. Perforation on the copper tape is nearly intact.

(b) Failure of perforated copper tape when it is pulled away. Polymer stake cuts through the copper tape thus tearing the tape beyond the hole.

Figure 7.3: Schematic of 2 possible failure points at the macro level interface between the copper-ETPU interlocking witin the polymer matrix.

geometrical estimation can be made about R_{3D}, in an attempt to estimate values of parasitic resistance R_{3D} and contact resistance $R-C$. L and W represent the length and width of the constituent, respectively.

From a geometrical standpoint, the parasitic resistance R_{3D} is considered to be almost negligible when compared to the constituent bulk resistance R_b. This is desired, in order to maximise the sensitivity to detect the contact resistance. This is also considered in Chapter 3, where the distance between adjacent copper tapes is minimized to directly reduce the parasitic contribution from the space between. Hence, implementing these assumptions into Equation 3.5, we obtain that $R_b \approx R_{4\text{-wire}}$.

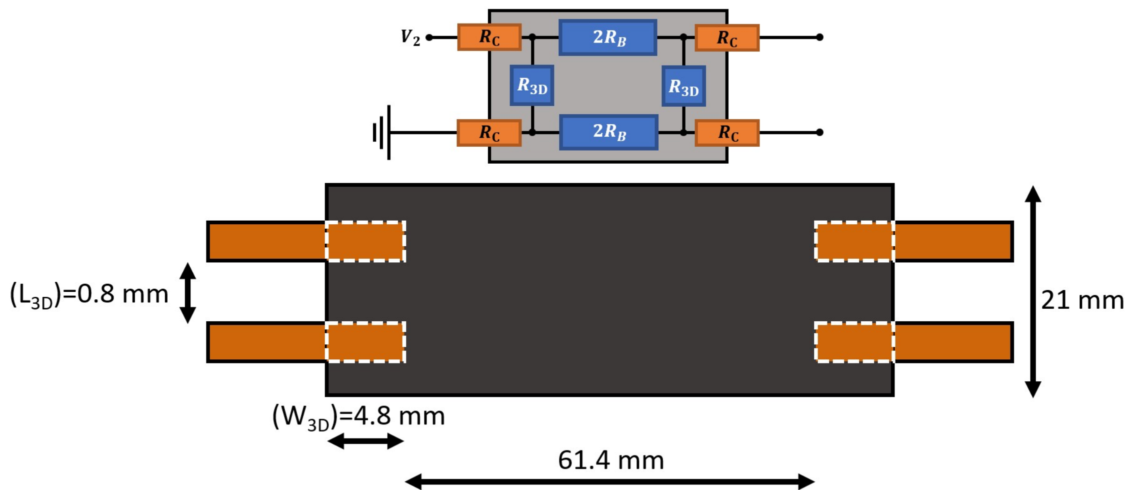

Figure 7.4: Schematic depicting the lumped model of the tape sample along with a geometrical model with dimensions labelled. The dotted lines indicate the region of the tape embedded within the ETPU layers.

$$R_{3D} \propto \frac{L_{3D}}{W_{3D}} = \frac{0.8\,\text{mm}/4.8\,\text{mm}}{61.4\,\text{mm}/21\,\text{mm}} R_b/2 = \frac{35}{1228} R_b \approx \frac{35}{1228} R_4 \tag{7.1}$$

From Figure 6.10 and other 3-wire and 4-wire resistance graphs obtained, $R_{4\text{-wire}} = 11.54\,\text{k}\Omega$ to $17.28\,\text{k}\Omega$ at $0\,\text{N}$ pulling force for tape samples from 0 to 20 holes. Using Equation 7.1, this estimation provides value for R_{3D} in the range of $329\,\Omega$ to $492\,\Omega$ [19].

Using Figure 6.10, values of $\Delta R_{3,4}$ are noted accordingly. We use Equation 3.9 and obtain values for contact resistance R_C lying in the range of 10.4 Ω to 426.45 Ω.

We use Equation 3.7 to obtain the value of bulk resistance R_b and verify these with the values of 4-wire resistance from the graphs obtained. This should provide us an idea about the validity of our assumption $R_b \approx R_{4\text{-wire}}$ from geometrical estimation [19].

$R_{4\text{-wire}}$ was found from the graphs to be ranging from 11.54 kΩ to 17.28 kΩ, whereas R_b was calculated to be ranging correspondingly from 11.77 kΩ to 17.38 kΩ. While there are disparities upto around 300 Ω, there must be further considerations of the assumptions taken in Equation 3.9, neglecting a remnant term $\frac{R_{3D}}{R_b}$. This can be studied and addressed in detail if an advanced approach takes the geometrical and electrical effects in a 3-dimensions into consideration. While contact resistance seems to be arguably larger for the wire samples, but this could be explained by a larger spacing between the copper tape and wire [19]. Producing a consistent wire sample to validate the results could be difficult without more sophisticated procedures for fabrication and embedding the wires into the polymer. Contact resistance only amounts to a few percentage of the sample resistance measured, thus definitely a modest indicator of the effectiveness of mechanical interlocking achieved by extruding polymer onto perforated copper tapes [19].

7.7 Behavior of resistance during pulling

The behavior of the resistance in both the measurements performed is quite interesting to look at. Alongside being influenced by the individual mechanical and electrical properties of the sample, it is also affected by the nature of the physical interlock and change in contact points at the interface due to specific type of loading. There could be more underlying reasons which have not be found yet.

In uniaxial loading, it has been observed that the resistance initially stays stable for a very short amount of time before ascending with increasing force, especially for the samples which did not break. As explained in subsection 7.4, the number of contact points between ETPU stake and copper tape has been theorized to vary with respect to their positions while remaining stationary and during pulling. Figure 7.5 depicts remnants of failed samples where the widened perforations can be observed.

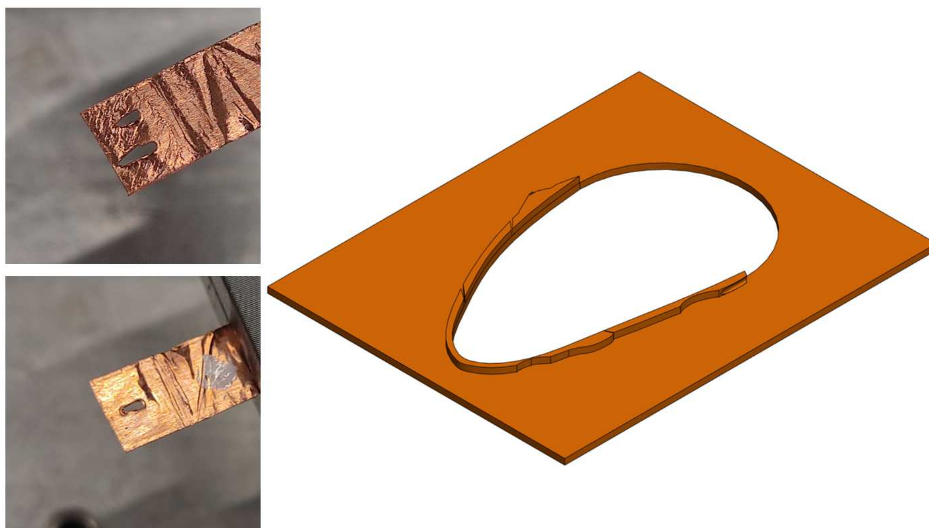

Figure 7.5: Closeup of copper tape after failure of the sample along with a schematic showing the ridges around the perforation.

This irregular widening can occur when the ETPU stake endures the pulling force, thus tearing away at the hole. This tear also leaves behind folds or ridges on the tape. Figure 7.5 also depicts a schematic on the left where these ridges are shown at the boundary of the hole.

The initial increase in resistance could potentially mean that the ETPU stake's contact with the copper tape could be reduced due to the widening of the perforation due to stronger loads. Figure 7.6 depicts what happens to the ETPU and copper tape when viewed from a marco and micro scale level. The gap on the tape depicted on the bottom left indicates the original perforation having slighly moved away from the ETPU stake due to the pulling force. When observed from a macro scale, tThe highlighted blue regions which signify contact points (asperities) would seemingly reduce by half due to lack of contact. At the micro scale, it can depend on the deformations of asperities and their combined contribution to effective contact area.

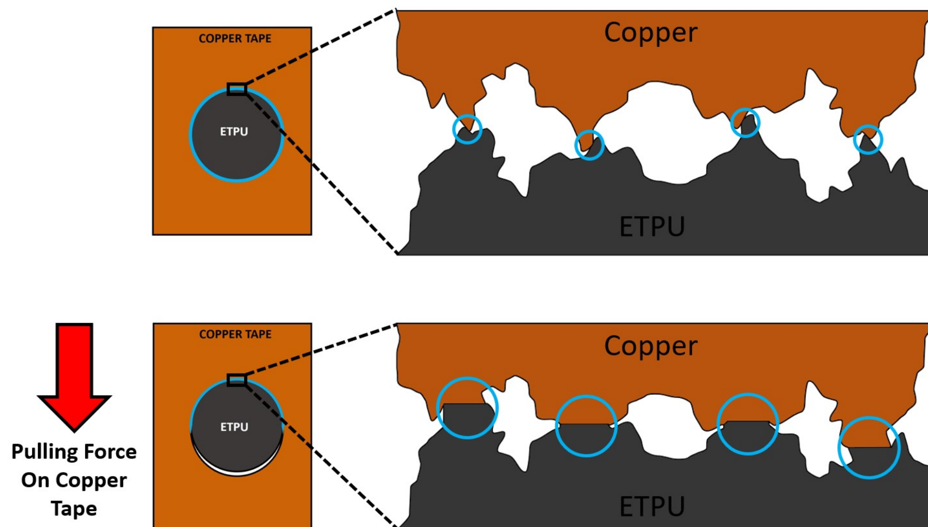

Figure 7.6: Schematic depicting the orientation of ETPU stake and copper tape along with their respective zoomed in view of contact points at the interface. The blue regions indicate the contacting points between both materials.

However, it can also be hypothesized that on the opposite side of the ETPU, effective contact area is seemingly increased. The resistance stabilizes and slowly decreases as force increases. This can possibly be explained due to the increased contact of the ETPU stake with the newly formed ridges on the tapes. This is considered in addition to the flattening of asperities as depicted in Figure 7.6 on the bottom right, due to the increased force. The larger blue circles depict the increased effective contact area occurring at the micro level when compared to the asperities on the top right. Greater effective contact area for conduction can directly influence and reduce the resistance. This combined effect from the ridges and flattened asperities could counteract the reduced contact on the other half of the ETPU's surface, which might explain why resistance is observed to reduce towards the end of the experiments. However, this reduction is also observed in the wire samples even without having effective interlocks with the polymer compared to tape samples. With the frayed structure of the embedded wires, there can still be some polymer seepage between individual wire strands which could amount to a weak form of mechanical interlocking. This is again a hypothesis, as there is no sure way of determining the pattern of frayed wires during extrusion of polymer onto it, which ended up fabricating samples with varying quality. Currently, producing wire samples with consistent quality remain a challenge with a lot of variables in procedure and human error, so this hypothesis might very well apply to this specific wire sample alone.

7.8 Conclusion

An in depth study towards establishing a reliable connection between ETPU and copper has provided valuable insights about the mechanical and electrical behavior of the sample. The results depict a nascent promise for utilizing perforated copper tape when compared to wires, for stronger mechanical bonding and lower electrical resistance. Role of optimizing perforations for enhancing performance is evident, but the study also highlights potential challenges such as structural weakening and the need for further investigation into long term stability. The discussion on thermal expansion disparity between ETPU and copper highlights the importance of considering material properties during design and optimization decisions. The influence of asperities between copper and polymer during pulling, helps in understanding the behavior of the connection under load. The behavior of resistance during load, characterized by its initial stability, subsequent and eventual stabilization or reduction, opens up avenues for further experimental testing. This discussion not only sheds light onto current findings but also sets the stage for future refinements and suggestions which could fortify the foundations laid in this research work, which is recommended in the next chapter, along with the conclusive remarks of the undertaken research.

8 Conclusion and Recommendations

8.1 Conclusion

The characterization and testing of mechanical interlocking to bond metals to 3D-printed polymeric conductors is investigated. After understanding the theoretical background of joining materials it is followed by an emphasis on utilizing mechanical interlocking to secure metals and polymers. This is further complemented by understanding the pioneering previous work done in this realm, which served as a foundation to build upon.

A thin block of ETPU polymer with four perforated copper tapes embedded within was designed as the test specimen. A lumped electrical model of this physical sample was an essential first step in the derivation of expressions for the contact and parasitic resistances of the system. This model is a simplified representation of the physical sample which also assumes the inherent properties are uniform and without variations, thus remains easy to implement. However, considering the 3 dimensional structure of the sample along with the environmental effects and further factors during loading is a necessary step in studying the behavior of contact resistance. Contact resistance is one of the main performance parameters whose behaviour is to be observed through testing.

Prior to testing, this designed sample was fabricated using FDM 3D printing and utilizing a custom-made punching jig to perforate the copper tapes. The printing parameters and hole patterns were optimized to achieve effective interlocking, electrical conduction and successful embedding of copper between polymer layers.

An experimental setup was designed and implemented around the sample, to measure the mechanical and electrical properties under uniaxial and cyclic tensile loads. This consisted of a clamp and base plate, which were custom built specifically to function as means of pulling and as the sample holder. This setup provided a way for simultaneously measuring the contact resistance while a tensile force is applied to the samples. These forces consisted of uniaxial and cyclic loading, to simulate potential real world applications. The behaviour of contact resistance and breaking points of copper tapes were observed. The results were analyzed and potential factors that influence the performance of the interlocking method were discussed. Some of these are the role of perforations, difference in thermal expansion coefficients between ETPU and copper along with the hypothesized effect of contact points between copper and polymer during loading and the copper tape failure mechanisms.

From the results obtained, a direct relation between number of holes and the contact resistance is not established [19]. The parasitic resistance term $R_{3D}/2$ is noted to be significant [19]. Ideally, this parasitic resistance is undesirable and further geometrical considerations can be implemented to further reduce this. But more importantly, it has been observed from the measurements that contact resistance remains relatively low and stable even under large periodic loads [19]. Upon taking more considerations in the future for the lumped model, further changes can be implemented into the design of samples, which can once more reduce the parasitic contribution of resistance. For an improved comprehension, there is a clear need for further experimentation along with being able to compare results with current sample designs [19].

Mechanical interlocking among perforated copper tapes can create mechanically stronger and more stable contacts than conventional wires, based on the tests performed. It should be worth noting that flexibility was indeed one of the persistent limitations of conventional methods like soldering, chemical adhesion or welding. The interlocking connections within these samples are considered to remain effective due to the change in thermal expansion coefficients between

copper and ETPU, which promotes shrink fit upon cooling which directly influences the real contact area between these materials.

This novel method initially explored by Neuvel [12], indeed has the potential to be applied in flexible, stretchable and conductive devices, as part of soft robotics and biomedical applications. Wearable sensors that measure physiological signals, robotic prostheses which emulate flexible limb behaviour like grasping and manipulation and skin/clothing integrated displays, to name a few.

In conclusion, this thesis has demonstrated the feasibility and effectiveness of interlocking metals and 3D-printed polymeric conductors, for establishing electrical contacts onboard flexible 3D-printed structures and leaves ample insights and suggestions for further advancements in this field.

8.2 Future Recommendation

It is clear that there are several ventures towards improving and standardizing mechanical interlocking as a reliable method in order to be employed in applications. One of the main limitations is the lack of more complex theoretical model that can better predict the contact resistance under different loading conditions. The corresponding expressions derived are based on a lumped electrical model that is fairly simple. It does not account for the complex multi-layered geometry along with the deformation of the copper tapes and ETPU. Moreover, the experimental setup and measurement techniques may have some sources of error and uncertainty that affect the reliability and validity of results. A more systematic and rigorous approach is necessary to find optimal parameters to maximize interlocking strength and electrical conductivity. In an overview, these are mostly around modelling, fabrication, improving the observation and accuracy of results along with suggestions that can carry this research forward.

- *Materials, geometry and print patterns*
  The samples used in this research were designed and fabricated taking considerations for testing and simplicity. Based on the various parameters involved, there is room for further optimization of design and print parameters, such as number, pattern and size of perforations on the copper tape, thickness and layers of ETPU layer, printing speed, alignment and mounting of tapes. Research can also be extended to explore different combinations of materials that could benefit this reliable and conductive connection corresponding to the applications.

  Utilizing a staggered hole pattern in place of an ortholinear one could result in potentially stronger interlocking. A staggered hole pattern on a metal surface makes it comparatively stronger than a surface with a ortholinear pattern [71]. Along with providing more even distribution of stress, staggered hole pattern possess wider open areas to perforate more holes [71], which could seemingly increase the number of interlocks.

  Extrusion print pattern of ETPU was rectilinear with a flow multiplier of 130% and infill density 100%. Newer patterns can be further explored amongst various samples and compared.

  Influential parameters can indeed affect the mechanical and electrical properties of the sample along with the reproducibility and reliability. This calls for a systematic study of the effects of these parameters on the interlocking mechanism and contact resistance, in order to find optimal values of each parameters and establish a standard protocol for fabrication and testing of the samples.

- *Design of jig*
  A jig similar to assistance tool can be designed to heat and systematically secure the tape onto the polymer matrix with fewer human errors with regards to positional placement.

Utilizing a soldering rod manually to produce consistent sample quality repeatedly is a challenge, thus could impact the results. A standardized and uniformly distributed form of heating can improve the interlock quality as the role played by the soldering rod is cardinal in securing the copper tape onto the polymer even prior to interlocking. A large heated plate can be ironed on the tape to distribute heat equally throughout and allowing for proximal polymer matter to be molten and smeared over.

Perforated copper tapes were also observed to have burrs still attached. These are adhered scrap material remnants after the punch is used. A sharper punch and a corresponding hole with lower tolerance can be used to avoid copper tape bending. Additionally, a stronger punching force can also be utilized. Burrs could also occur if the punching angle is not completely perpendicular. A slight angle change from human influences can be eliminated with a design update or utilizing a designated machine.

- *Experiment and measurement*
  To validate the reliability and reproducibility of the novel method, a greater number of samples need to be tested along with different hole configurations and tape geometries. This is also a statistical analysis of the contact resistance and breaking force data from across multiple runs can help identify the significance and variability of the results.

  Greater force magnitudes can be considered for testing can be considered to study the durability and fatigue behavior of contacts greater force application to study breaking points during cyclic loading in order to also obtain insight into the behavior of resistance during loading and unloading cycles.

  To explain the observed behavior of the 4-wire resistance, which showed how it decreased, increased and again slightly decreased with increasing force, a possible hypothesis is the piezoresistive effect of the EPTU material. This effect refers to the change in electrical resistance due to mechanical deformation.

  To measure the contact resistance more effectively, a different setup should be designed to reduce the parasitic resistance $R_{3\mathrm{D}}$. Currently this resistance is quite significant, with the piezoresistive effect bringing changes due to pulling. A different sample geometry or electrode layout can also be explored to reduce the the effect of the parasitic resistance.

- *Observation*
  So far, destructive observation was employed to study the anatomy and obtain information insight about the quality of the contact. Due to this, any specific sample's behavior to loading conditions cannot not be determined. A non-destructive way to observe the contact quality could help in obtaining reliable results during testing. A sample's interlock quality could be directly related to its performance under load. This form of observation could also provide clues for the potential voids observed in polymer matrix within the immediate proximity of the copper regions. Further implementation of this could help in simultaneous observation of the interface during polymer extrusion, solidification and loading conditions.

  Analysis of the failure point can be improved by taking a 3 dimensional consideration of the interior of the sample into account. This can help to model the stress distribution and current flow within the sample.

A Appendix 1

During the preparation of this work the author used OpenAI's ChatGPT 3.5 in order to improve the quality of writing with the aim to enhance readability & articulation and to obtain a preliminary idea for the skeletal structure of various sections of the report.

Critical analyses, inferences and conclusions remain solely drawn by the author.

After using this tool/service, the author reviewed and edited the content as needed and takes full responsibility for the content of the work.

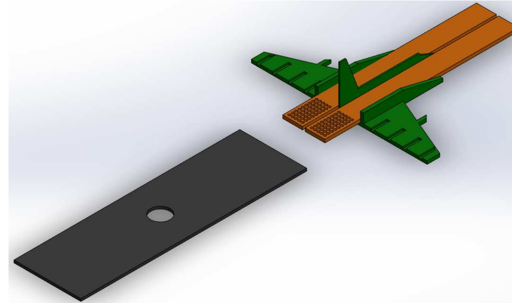

Figure A.1: Copper tapes mounted on the assistance tool with the perforated region lying outside the tool. The polymer block and the assistance tool are both lying on the heated printed bed as depicted in the white.

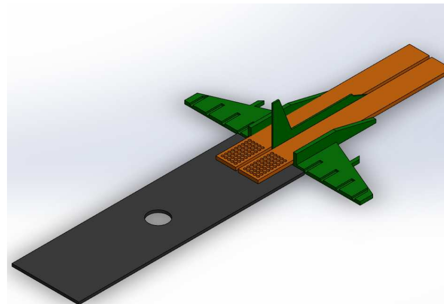

Figure A.2: The markers on the wings are utilized to bring the assistance tool closer in order to place the perforated region of the copper tape onto the polymer block. The copper tapes do not stick to the surface.

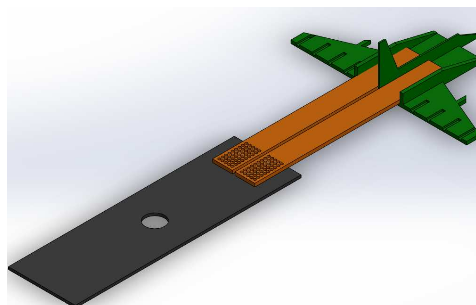

Figure A.3: The tool is pulled away, leaving behind adjacent copper tapes secured onto the half printed polymer block.

Bibliography

[1] O. A. Mohamed, S. H. Masood, and J. L. Bhowmik, “Optimization of fused deposition modeling process parameters: a review of current research and future prospects,” *Adv. Manuf.*, vol. 3, pp. 42–53, Mar. 2015.

[2] M. Saari, B. Cox, E. Richer, *et al.*, “Fiber encapsulation additive manufacturing: An enabling technology for 3d printing of electromechanical devices and robotic components,” *liebertpub.com*, vol. 2, pp. 32–39, Mar. 2015.

[3] N. Lu and D. H. Kim, “Flexible and stretchable electronics paving the way for soft robotics,” *Soft Robot.*, vol. 1, pp. 53–62, Mar. 2014.

[4] E. Aguilera, J. Ramons, D. Espalin, F. Cedillos, D. Muse, R. WIcker, and E. MacDonald, “3d printing of electro mechanical systems,” *2013 International Solid Freeform Fabrication Symposium*, 2013.

[5] R. Kwok, “Neuroprosthetics: Once more, with feeling,” *Nature*, vol. 497, pp. 176–178, 2013.

[6] M. Stoppa and A. Chiolerio, “Wearable electronics and smart textiles: A critical review,” *Sensors*, vol. 14, no. 7, pp. 11957–11992, 2014.

[7] J. T. Muth *et al.*, “Embedded 3d printing of strain sensors within highly stretchable elastomers,” *Advanced Materials*, vol. 26, pp. 6307–6312, Sep. 2014.

[8] H. Watschke, K. Hilbig, and T. Vietor, “Design and characterization of electrically conductive structures additively manufactured by material extrusion,” *Applied Sciences*, vol. 9, p. 779, 02 2019.

[9] N. Lazarus and S. Bedair, “Creating 3d printed sensor systems with conductive composites,” *Smart Materials and Structures*, vol. 30, p. 015020, 01 2021.

[10] H. Nassar and R. Dahiya, “Fused deposition modeling-based 3d-printed electrical interconnects and circuits,” *Advanced Intelligent Systems*, vol. 3, 09 2021.

[11] M. Revilla-León, M. Meyer, A. Zandinejad, and M. Özcan, “Additive manufacturing technologies for processing zirconia in dental applications. a literature review on current status and future perspective.,” *International journal of computerized dentistry*, vol. 23, pp. 27–37, 03 2020.

[12] P. Neuvel, “Developing a reliable method to connect conductors to 3d printed conducting structures,” August 2020. http://essay.utwente.nl/83047/.

[13] K. Martinsen, S. J. Hu, and B. E. Carlson, “Joining of dissimilar materials,” *CIRP Annals - Manufacturing Technology*, pp. 679–699, 2015.

[14] S. T. Amancio-Filho and L.-A. Blaga, eds., *Joining of Polymer-Metal Hybrid Structures: Principles and Applications.* John Wiley & Sons, Inc, feb 2018.

[15] G. Dumstorff, S. Paul, and W. Lang, “Integration without disruption: The basic challenge of sensor integration,” *IEEE Sensors Journal*, vol. 14, no. 7, pp. 2102–2111, 2014.

[16] M. Schouten, C. Spaan, D. Kosmas, R. Sanders, and G. Krijnen, “3d printed capacitive shear and normal force sensor using a highly flexible dielectric,” in *2021 IEEE Sensors Appl. Symp. SAS 2021 - Proc.*, August 2021.

[17] A. Dijkshoorn, M. Schouten, G. Wolterink, R. Sanders, S. Stramigioli, and G. Krijnen, "Characterizing the electrical properties of anisotropic, 3d-printed conductive sheets for sensor applications," *IEEE Sensors Journal*, vol. 20, no. 23, pp. 14218–14227, 2020.

[18] R. Freund, S. Koch, H. Watschke, E. Stammen, T. Vietor, and K. Dilger, "Utilization of additively manufactured lattice structures for increasing adhesive bonding using material extrusion," 2021.

[19] A. Dijkshoorn, V. Ravi, P. Neuvel, S. Stramigioli, and G. Krijnen, "Mechanical interlocking for connecting electrical wires to flexible, fdm, 3d-printed conductors," in *2022 IEEE International Conference on Flexible and Printable Sensors and Systems (FLEPS)*, pp. 1–4, 2022.

[20] P. Viswanadham, "Role of adhesion and its reliability implications in electronic assemblies," in *4th International Conference on Adhesive Joining and Coating Technology in Electronics Manufacturing. Proceedings. Presented at Adhesives in Electronics 2000 (Cat. No.00EX431)*, pp. 28–34, 2000.

[21] A. Baldan, "Adhesion phenomena in bonded joints," *International Journal of Adhesion and Adhesives*, vol. 38, p. 95–116, 10 2012.

[22] A. Baldan, "Adhesively-bonded joints and repairs in metallic alloys, polymers and composite materials: Adhesives, adhesion theories and surface pretreatment," *Journal of Materials Science*, vol. 39, pp. 1–49, 01 2004.

[23] A. International, "Astm international - astm d907-1, standard terminology of adhesives," p. 13, 2015.

[24] F. Awaja, M. Gilbert, G. Kelly, B. Fox, and P. J. Pigram, "Adhesion of polymers," *Progress in Polymer Science*, pp. 948–968, 2005.

[25] L. H. Sharpe and H. Schonhorn, *Surface Energetics, Adhesion, and Adhesive Joints*, ch. 12, pp. 189–201. 1964.

[26] B. V. Derjaguin and V. P. Smilga, "Electronic theory of adhesion," *Journal of Applied Physics*, vol. 38, pp. 4609–4615, 1963.

[27] D. A. Dillard, A. V. Pocius, and M. Chaudhury, *The Mechanics of Adhesion*. Elsevier, Amsterdam, second ed., 2002.

[28] M. Deruelle, M. Tirrell, Y. Marciano, H. Hervet, and L. Léger, "Adhesion energy between polymer networks and solid surfaces modified by polymer attachment," *Faraday Discuss.*, vol. 98, pp. 55–65, 1994.

[29] J. W. McBain and D. G. Hopkins, "On adhesives and adhesive action," *The Journal of Physical Chemistry*, vol. 29, pp. 188–204, 1925.

[30] G. Carbone and F. Bottiglione, "Asperity contact theories: Do they predict linearity between contact area and load?," *Journal of the Mechanics and Physics of Solids*, vol. 58, pp. 2555–2572, 2008.

[31] A. Emami, S. Khaleghian, and S. Taheri, "Asperity-based modification on theory of contact mechanics and rubber friction for self-affine fractal surfaces," *Friction*, vol. 9, pp. 1707–1725, 2021.

[32] C. Zhai, A. H. H. Dorian, G. Proust, L. Brassart, and T. Gan, "Interfactial electro-mechanical behavior at rough surfaces," *Extreme Mechanics Letters*, vol. 9, pp. 422–429, 2016.

[33] R. Messler, "Joining of materials and structures: From pragmatic process to enabling technology," pp. 1–790, 08 2004.

[34] A. J. Petty II, R. L. Keate, B. Jiang, G. A. Ameer, and J. Rivnay, "Conducting polymers for tissue regeneration in vivo," *Chemistry of Materials*, vol. 32, pp. 4095–4115, 2020.

[35] P. Kah, R. Suoranta, J. Martikainen, and C. Magnus, "Techniques for joining dissimilar materials: Metals and polymers," *Reviews on Advanced Material Science*, pp. 152–164, 2013.

[36] Y. Xie, J. Zhang, and T. Zhou, "Large-area mechanical interlocking via nanopores: Ultrahigh-strength direct bonding of polymer and metal materials," *Applied Surface Science*, vol. 492, pp. 558–570, 2019.

[37] S. Ji and X. Chen, "Enhancing the interfacial bonding strength between modular stretchable electronic components," *National Science Review*, 2022.

[38] Z. Liu, X. Wang, D. Qi, C. Xu, J. Yu, Y. Liu, Y. Jiang, and B. Liedberg, "High-adhesion stretchable electrodes based on nanopile interlocking," *Advanced Materials*, vol. 29, p. 1603382, 2016.

[39] L. H. Sperling, *Multicomponent Polymeric Materials*, ch. 13, pp. 687–756. John Wiley & Sons, Ltd, 2005.

[40] R. R. Ma, J. T. Belter, and A. M. Dollar, "Hybrid deposition manufacturing: Design strategies for multimaterials mechanisms via three -dimensional printing and material deposition," *Journal of Mechanisms and Robotics*, vol. 7, p. 021002, 2015.

[41] Y. Park, H. Luan, K. Kwon, S. Zhao, D. Franklin, H. Wang, H. Zhao, W. Bai, K. J. Uk, W. Lu, J.-H. Kim, Y. Huang, Y. Zhang, and J. A. Rogers, "Transformable, freestanding 3d mesostructures based on transient materials and mechanical interlocking," *Advanced Functional Materials*, vol. 29, 2019.

[42] S. Erol and G. Rajesh, "A study on the effects of surface roughness on the strength of single lap joints," *Jounrla of Adhesion Science and Technology*, vol. 15, p. 97, 2001.

[43] P. A. Fabrin, M. E. Hoikkanen, and J. E. Vuorinen, "Adhesion of thermoplastic elastomer on surface treated aluminum by injection molding," *Polymer Engineering & Science*, vol. 47, pp. 1187–1191, 2007.

[44] F. Kimura, S. Kadoya, and Y. Kajihara, "Effects of molding conditions on injection molded direct joining using a metal with a nano-structured surface," *Precision Engineering*, vol. 45, pp. 203–208, 2016.

[45] S. C. Han, L. H. Wu, C. Y. Jiang, N. Li, C. L. Jia, P. Xue, H. Zhang, H. B. Zhao, D. R. Ni, B. L. Xiao, and Z. Y. Ma, "Achieving a strong polypropylene/aluminium alloy friction spot joint via a surface laser processing pretreatment," *Journal of Materials Science & Technology*, vol. 50, pp. 103–114, 2020.

[46] S. Aliasghari, M. Ghorbani, P. Skeldon, H. Karami, and M. Mohavedi, "Effect of plasma electrolytic oxidation on joining of aa 5052 aluminium allot to polypropylene using friction stir spot welding," *Surface and Coatings Technology*, vol. 313, pp. 274–281, 2017.

[47] O. O. Ojo, "Macro-/micro-mechanical interlocking modification on the performance of hybrid friction stir spot welded aluminium/acrylonitrile butadiene styrene joints," *Research on Engineering Structures & Materials*, vol. 7, pp. 617–633, 2021.

[48] M. Paidar, O. O. Ojo, M. Amirhossein, H. K. Pabandi, and M. Elsa, “Pre-threaded hole friction stir spot welding of aa2219/pp-cs0s sheets,” *Journal of Materials Processing Technology*, p. 116272, 2019.

[49] H. K. Pabandi, M. Movahedi, and A. H. Kokabi, “A new refill friction spot welding process for aluminium/ polymer composite hybrid structures,” *Composite Structures*, vol. 174, pp. 59–69, 2017.

[50] S. Zhao, F. Kimura, S. Kadoya, and Y. Kajihara, “Experimental analysis on mechanical interlocking of metal-polymer direct joining,” *Precision Engineering*, vol. 61, pp. 120–125, 2020.

[51] Y. Kajihara, Y. Tamura, F. Kimura, G. Suzuki, N. Nakura, and E. Yamaguchi, “Joining strength dependence on molding conditions and surface textures in blast-assisted metal-polymer direct joining,” *CIRP Annals*, vol. 76, pp. 591–594, 2018.

[52] X. Li, F. Liu, N. Gong, P. Huang, and C. Yang, “Enhancing the joining strength of injection-molded polymer-metal hybrids by rapid heating and cooling,” *Journal of Materials Processing Technology*, vol. 249, pp. 386–393, 2017.

[53] Protopasta, “Electrically conductive composite pla.” `https://www.proto-pasta.com/products/conductive-pla`, accessed on 19.12.2023.

[54] Ninjatek, “Ninjaflex 3d printer filament tpu.” `https://ninjatek.com/shop/ninjaflex/`, accessed on 19.12.2023.

[55] M. Schouten, “Towards additively manufactured complex robotic systems,” 2017.

[56] G. Dumstorff and W. Lang, “Investigations on the impact of material-integrated sensors with the help of fem-based modeling,” *Sensors*, vol. 15, no. 2, pp. 2336–2353, 2015.

[57] C. M. Gheorghiţă, M. Adam, M. Andruşcă, A. Munteanu, and A. Dragomir, “About contact resistance of the electrical equipment,” in *2017 International Conference on Modern Power Systems (MPS)*, pp. 1–4, 2017.

[58] S. J. Proctor, Loren, Linhom, and J. A. Mazer, “Direct measurements of interfacial contact resistance, end contact resistance, and interfacial contact layer uniformity,” *IEEE Transactions on Electron Devices*, vol. 30, pp. 1535–1542, 1983.

[59] H. Berger, “Contact resistance and contact resistivity,” *Journal of The Electrochemical Society*, vol. 119, pp. 507–514, 1972.

[60] A. Dragomir, M. Adam, M. Andruşcă, M. Molodeschi, and R. Pantelimon, “About thermal stresses monitoring and diagnosis of electrical equipment,” in *2014 International Conference and Exposition on Electrical and Power Engineering (EPE)*, pp. 289–294, 2014.

[61] M. Andruşcă, M. Adam, R. Burlica, A. Munteanu, and A. Dragomir, “Considerations regarding the influence of contact resistance on the contacts of low voltage electrical equipment,” in *2016 International Conference and Exposition on Electrical and Power Engineering (EPE)*, pp. 123–128, 2016.

[62] W.-b. Ren, D. Du, and Y. Du, “Electrical contact resistance (ecr) of connector response to mechanical vibration environment,” *IEEE Transactions on Components, Packaging and Manufacturing Technology*, vol. PP, pp. 1–1, 08 2019.

[63] R. Fu, S. Choe, R. Jackson, G. Flowers, M. Bozack, L. Zhong, and D. Kim, "Vibration-induced changes in the contact resistance of high power electrical connectors for hybrid vehicles," *Components, Packaging and Manufacturing Technology, IEEE Transactions on*, vol. 2, 02 2012.

[64] H. Laurila, "Resistance measurement; 2, 3 and 4 wire connection." https://blog.beamex.com/resistance-measurement-2-3-or-4-wire-connection, accessed on 19.12.2023.

[65] J. Janesch, "Two-wire vs. four-wire resistance measurements: Which configuration makes sense for your application?." https://assets.testequity.com/te1/Documents/ARTICLE_LIBRARY/Keithley%20-Two-Wire%20vs%20Four-Wire%20Resistance%20Measurements.pdf, accessed on 19.12.2023.

[66] 3M, "3m™ copper foil tape 1181 data sheet." https://www.farnell.com/datasheets/2340440.pdf, last accessed on 19.12.2023.

[67] "Rubber 3d printing." https://rubber3dprinting.com/, accessed on 19.12.2023.

[68] Ultimaker, "Ultimaker tough pla - 2.85 mm - 750 g - white." https://www.3dprima.com/filaments/ultimaker-tough-pla-2-85-mm-750-g-white_24684_5781, accessed on 19.12.2923.

[69] UltiMaker, "Ultimaker s3." https://ultimaker.com/3d-printers/ultimaker-s3, accessed on 19.12.2023.

[70] UltiMaker, "Pla for s series." https://ultimaker.my.salesforce.com/sfc/p/#j0000000HOnW/a/5b000007wU1H/7QMjxlrYpKAatX_WPUJfojZ.kaw_5tK33flGPAlSUtc, accessed on 19.12.2923.

[71] "Designers, specifiers & buyers handbook for perforated metals," 1993. https://www.marcospecialtysteel.com/content/uploads/2017/01/Perforated-Handbook-for-designers-min.pdf, last accessed on 19.12.2023.